

## Advanced imaging techniques for assessment of structure, composition and function in biofilm systems

Thomas R. Neu<sup>1</sup>, Bertram Manz<sup>2</sup>, Frank Volke<sup>2</sup>, James J. Dynes<sup>3,4</sup>, Adam P. Hitchcock<sup>3</sup> & John R. Lawrence<sup>4</sup>

<sup>1</sup>Department of River Ecology, Helmholtz Centre for Environmental Research – UFZ, Magdeburg, Germany; <sup>2</sup>Fraunhofer Institute for Biomedical Engineering (IBMT), St. Ingbert, Germany; <sup>3</sup>CLS – CCRS, McMaster University, Hamilton, ON, Canada; and <sup>4</sup>Environment Canada, Saskatoon, Saskatchewan, Canada

**Correspondence:** Thomas R. Neu, Department of River Ecology, Helmholtz Centre for Environmental Research – UFZ, Brueckstrasse 3a, 39114 Magdeburg, Germany. Tel.: +49 391 8109 800; fax: +49 391 8109 150; e-mail: thomas.neu@ufz.de

Received 31 October 2008; revised 30 November 2009; accepted 24 December 2009. First version published online 18 February 2010.

DOI:10.1111/j.1574-6941.2010.00837.x

Editor: Ian Head

### Keywords

biofilms; imaging; microscopy; laser scanning microscopy (LSM); magnetic resonance imaging (MRI); scanning transmission X-ray microscopy (STXM).

### Introduction

Imaging techniques are a major research tool used to investigate and understand complex structures and processes in various scientific disciplines. Especially in the biological and medical fields, imaging has become an indispensable technique for noninvasive, three-dimensional examination of samples and objects at different spatial scales. The orders of magnitude examined range from nanometres (macromolecules), to micrometres (cellular level, microbial aggregates, biofilms) up to centimetres (microbial mats, tissue, organs, human body).

Magnification glasses and simple optical microscopes were the first tools that provided access to the new microscopic dimension. The first light microscope was used by Hook already in 1665. A few years later, Leeuwenhoek was looking at microbiological samples; in fact, he was the first to examine oral biofilms (Wainwright, 2003). For several hundred years, traditional light microscopy and its derivations have been the major tool for the observation and

### Abstract

Scientific imaging represents an important and accepted research tool for the analysis and understanding of complex natural systems. Apart from traditional microscopic techniques such as light and electron microscopy, new advanced techniques have been established including laser scanning microscopy (LSM), magnetic resonance imaging (MRI) and scanning transmission X-ray microscopy (STXM). These new techniques allow *in situ* analysis of the structure, composition, processes and dynamics of microbial communities. The three techniques open up quantitative analytical imaging possibilities that were, until a few years ago, impossible. The microscopic techniques represent powerful tools for examination of mixed environmental microbial communities usually encountered in the form of aggregates and films. As a consequence, LSM, MRI and STXM are being used in order to study complex microbial biofilm systems. This mini review provides a short outline of the more recent applications with the intention to stimulate new research and imaging approaches in microbiology.

examination of biological samples. In the last century, it was thought that the development of light microscopy was in its final stages. However, the invention of laser scanning microscopy (LSM) in the 1980s caused a revolution in light microscopy. More recently, the invention of stimulated emission depletion (STED) laser microscopy led to another major improvement in laser microscopy (Klar *et al.*, 2000). The second major invention in microscopy was electron microscopy by Knott and Ruska in 1931. Electron microscopy in the transmission and scanning mode allowed a higher magnification of fixed and dehydrated samples, and in combination with specific detectors, analysis of the elemental composition in specific regions of the sample. In 1982, Binning and Rohrer invented the scanning tunnelling microscope (Binning *et al.*, 1982). This microscope provided a convenient method to image atoms at surfaces. In the meantime, several variations have been developed that allow the analysis and manipulation of samples at the nanometre level. The phenomenon of nuclear magnetic

resonance (NMR) was discovered by Bloch and Purcell in 1946 (Bloch *et al.*, 1946; Purcell *et al.*, 1946). Nevertheless, it took until 1973 to develop NMR imaging, when Lauterbur and Mansfield demonstrated independently that the application of magnetic field gradients can be used to obtain nuclear spin density images of a sample (Lauterbur, 1973; Mansfield & Grannell, 1973). This discovery was the basis of a whole new field of research called magnetic resonance imaging (MRI). In 1895, Röntgen discovered X-rays and produced the first image of a hand, demonstrating X-rays' imaging potential. However, due to the lack of suitable X-ray sources, it was only in the modern era of third-generation synchrotron light sources starting in the 1990s that the source properties were compatible with X-ray microscopes suitable for high-resolution imaging and spectroscopy. Soft X-ray scanning transmission X-ray microscopy (STXM), an X-ray absorption technique, has since developed and provides chemical and biochemical information on biological and environmental samples through the collection of image sequences.

The purpose of this mini review is to provide a brief introduction to three specific advanced *in situ* imaging techniques – LSM, MRI and STXM (Table 1) – and to illustrate their applications in microbiology. As microbial communities commonly exist in the form of aggregates and films, specific focus is placed on the application of these techniques to hydrated microbial biofilm systems.

## LSM

### Variations of LSM

Since the first publication in the field of microbiology in 1991, LSM has developed into an important and indispensable tool for three-dimensional *in situ* imaging of microbial communities (Lawrence *et al.*, 1991). Despite this fact, numerous publications only partially took advantage of the large potential offered by advanced LSM. Frequently, the technique has been and still is used for the production of a colourful image only. Thus, what is meant by advanced LSM? Generally speaking, the LSM technique is used for three reasons: (1) visualization of multiple features in different channels and spectrally resolved, (2) analysis of structure, composition, microhabitats, activity and processes using a variety of specific probes and (3) volumetric and structural quantification of multichannel signals in four dimensions. More specifically, the LSM technique may be performed in a variety of ways. Firstly, the system can be equipped with lasers using one-photon excitation. This can be achieved using continuous UV and visible lasers or very recently white lasers also known as super-continuum light sources. The LSM technique is then usually called confocal laser scanning microscopy (CLSM). Secondly, the system, especially the newer fully equipped ones, can be set up with a laser using two-photon excitation (pulsed infrared laser).

**Table 1.** Major characteristics of LSM, MRI and STXM

Technique	Advantages	Limitations
LSM	<ul style="list-style-type: none"> <li>–Living, fully hydrated samples</li> <li>–Multichannel (up to 5) analysis</li> <li>–Noninvasive optical sectioning</li> <li>–Reflection and fluorescence mode</li> <li>–One-photon/two-photon excitation</li> <li>–Intensity and lifetime imaging</li> <li>–Three-dimensional analysis of macromolecules, cells, communities</li> <li>–Information on structure, processes and microhabitats</li> <li>–Extensive range of associated analytical tools</li> </ul>	<ul style="list-style-type: none"> <li>–Probe dependent (except for autofluorescence and GFP)</li> <li>–Depth of laser penetration due to absorption and scattering</li> <li>–Resolution if extreme differences of fluorescence emission intensity in one channel</li> </ul>
MRI	<ul style="list-style-type: none"> <li>–Probe independent</li> <li>–Living, fully hydrated samples</li> <li>–Noninvasive</li> <li>–Information about chemical species</li> <li>–Imaging of hydrodynamics</li> <li>–Various methods of contrast</li> </ul>	<ul style="list-style-type: none"> <li>–Limited resolution &gt; 1000 <math>\mu\text{m}^3</math></li> <li>–Slow</li> <li>–No ferromagnetic objects allowed</li> </ul>
STXM	<ul style="list-style-type: none"> <li>–Probe independent</li> <li>–Elemental analysis of inorganic and organic constituents</li> <li>–Speciation (molecular structure) from near-edge spectra</li> <li>–Quantitative mapping of chemical species &lt; 30 nm resolution</li> <li>–Fully hydrated samples</li> <li>–Orientation imaging from linear polarization signals</li> <li>–Tomographic imaging</li> </ul>	<ul style="list-style-type: none"> <li>–Synchrotron and beam time necessary</li> <li>–Wet mount between two fragile silicon nitride windows</li> <li>–Maximum samples thickness 300 nm</li> <li>–Maintaining full hydration can be challenging</li> <li>–Radiation damage</li> <li>–Absorption saturation</li> </ul>

This technique is known as two-photon or multiphoton laser scanning microscopy (2PLSM).

All the LSM applications described so far record the intensity of fluorescence signals. However, the fluorescence signal contains two pieces of information. In addition to the intensity, the lifetime of an excited fluorochrome can be measured in a technique known as fluorescence lifetime imaging. This approach opens up a range of new possibilities in the analysis of microbial communities (Neu *et al.*, 2004a, b; Neu & Lawrence, 2005; Walczysko *et al.*, 2008). The combination of fluorescence staining techniques, CLSM, 2PLSM, intensity imaging and lifetime imaging offers a wealth of opportunities in order to collect multiple pieces of information from highly complex biological systems such as microbial biofilms.

Imaging nowadays implies that the data are recorded and available in digital format. In this respect, an often neglected field is quantitative three-dimensional digital image analysis (DIA) of multichannel data sets. DIA includes not only visualization but also quantification of volumetric and structural constituents. In terms of volumetric information, deconvolution represents a major point of discussion. In light and laser microscopy, deconvolution is used to sharpen images and to harmonize the unequal resolution in the plane (*XY*) and depth (*Z*) directions. Nevertheless, deconvolution has been applied in only a few microbiological studies (Verity *et al.*, 1996; Phipps *et al.*, 1999; Manz *et al.*, 2000). The reason may lie in the constraints of performing deconvolution properly. This requires high-resolution imaging, which is impractical for routine work. DIA software can be divided into those primarily for visualization and those for quantification. Visualization of three-dimensional data sets seems to be straightforward, and several commercial software packages are available. Quantification is more difficult and consequently several research groups in microbiology developed their own programs matching their specific needs. One general program developed at the National Institute of Health called IMAGEJ is rather popular as it is freely available and useful in many research fields. More specific programs include, for example COMSTAT for flow cell biofilm microcolonies, PHILIP for phototrophic biofilms, DAIME for fluorescence *in situ* hybridization (FISH)-stained samples as well as ISA-3D for structural analysis and CONAN for imaging, structural analysis and quantification (see Table 2 for www sources). All the programs are very

different in terms of their runtime environment, file format acceptance, thresholding procedures, pixel/voxel/object recognition, volumetric quantification, colocalization analysis, determination of structural parameters and automation.

Because of the potential of LSM and more frequent availability of instruments, the number of CLSM manuscripts published in microbiology has increased exponentially. In this review, we will therefore provide a general overview and focus only on the major applications.

### Structure of microbial communities

The main application of LSM comprises the structural examination of biofilms and bioaggregates. Most importantly, LSM imaging has revealed the overall three-dimensional and internal structures of biofilms including voids and channels, which resulted in a new concept of biofilm architecture. Imaging of extracellular polymeric substances (EPS) has also extended our understanding of this important but understudied component of biofilms. As a consequence, LSM has kindled the interest in the role of the EPS matrix in biofilms. In addition, the digital image data sets are amenable to DIA including quantification. In order to start the analysis of a new and unknown microbiological sample, a structured approach has been suggested (Neu & Lawrence, 2002). This approach takes advantage of intrinsic biofilm properties such as reflection. This allows putting cells into the context of their microhabitat and, in addition, it allows imaging of reflective cell constituents, for example sulphur granules (Hinck *et al.*, 2007). Another intrinsic property especially of phototrophic biofilms is the autofluorescence, which can be used for imaging and differentiation (Neu *et al.*, 2004b). At the same time, the autofluorescence signal is needed as a control and for selecting the appropriate fluorescence stains. In combination with fluorescent probes specific for biofilm structural components, microbiological processes and microhabitats, a step by step, more complete impression of biofilm composition and functionality can be recorded. The most frequently used fluorochromes are nucleic acid-specific stains. Apart from the traditional fluorochromes, for example acridine orange and 4',6-diamidin-2-phenylindole, there are now many options of cell-permeable and cell-impermeable stains with different excitations and emissions (e.g. the Syto<sup>TM</sup> series). Details of

**Table 2.** Software available for digital image analysis of LSM data sets recorded from biofilm systems

Program	Application	Source
IMAGEJ	General image analysis	<a href="http://rsbweb.nih.gov/ij/">http://rsbweb.nih.gov/ij/</a>
COMSTAT	Flow cell biofilms	<a href="http://www.dtu.dk/centre/CSM/English/Instrument%20Center/Resources/COMSTAT%20Software.aspx">http://www.dtu.dk/centre/CSM/English/Instrument%20Center/Resources/COMSTAT%20Software.aspx</a>
PHILIP	Phototrophic biofilms	<a href="http://sourceforge.net/projects/phlip/">http://sourceforge.net/projects/phlip/</a>
DAIME	FISH analysis	<a href="http://www.microbial-ecology.net/daime/">http://www.microbial-ecology.net/daime/</a>
ISA-3D	Biofilm structural analysis	Lewandowski & Beyenal (2007)
CONAN	Biofilm imaging and structural analysis	<a href="http://www.biocom-online.de/index.html">http://www.biocom-online.de/index.html</a>

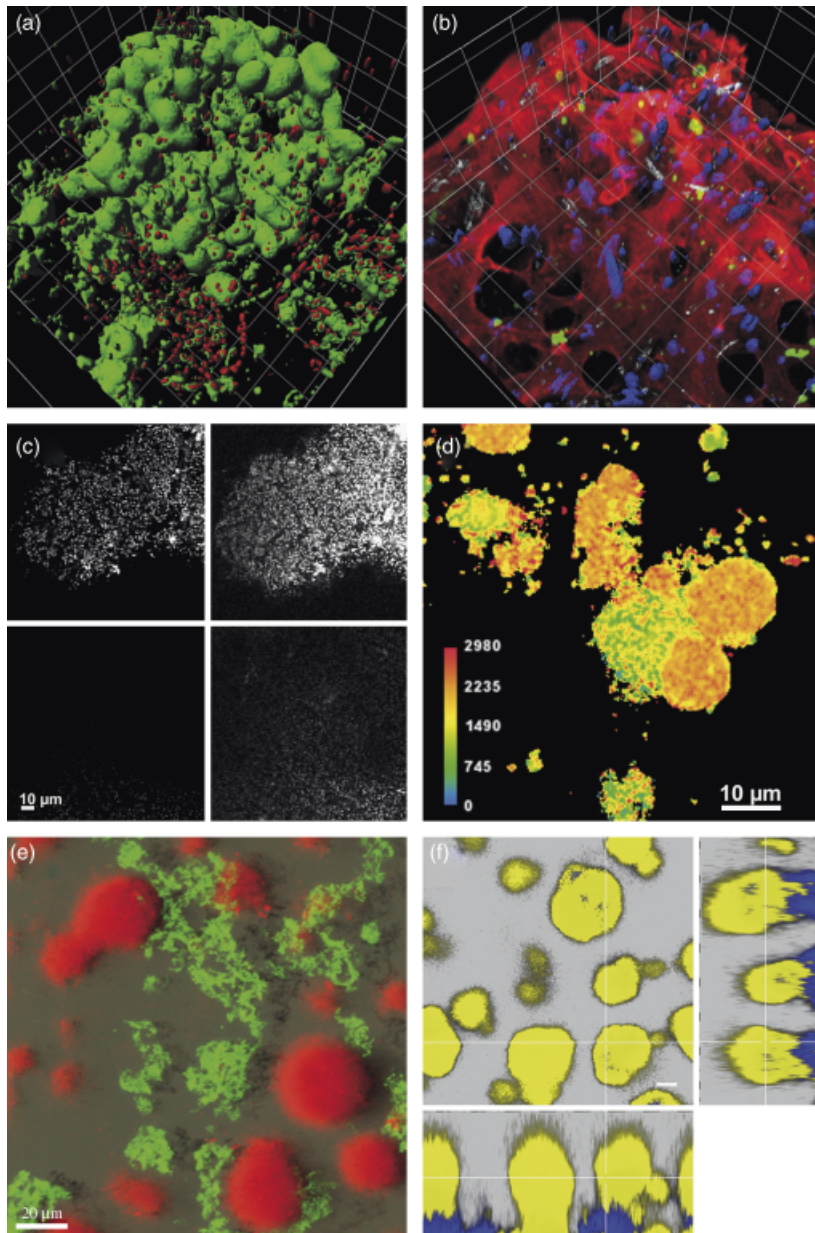


**Fig. 1.** Selection of different LSM approaches for structural examination of biofilm systems, including confocal, two-photon, lifetime imaging and GFP technique. (a) Two channel isosurface projection of a wastewater reactor biofilm after staining for glycoconjugates (*Aleuria aurantia* Alexa488 lectin = green) and counter-stained using the nucleic acid-specific fluorochrome Syto60 = red. Grid size = 10  $\mu\text{m}$ . (Image courtesy of Christian Staudt, UFZ, Magdeburg.) (b) Four-channel combined volume and isosurface projection of a phototrophic biofilm developed in a flow lane reactor. Colour allocation: autofluorescence of chlorophyll *a* = blue, *A. aurantia* Alexa488 lectin = red, *Artocarpus integrifolia* FITC lectin = green, reflection signal = white. Grid size = 20  $\mu\text{m}$ . (Image courtesy of Barbara Zippel, UFZ Magdeburg.) (c) Comparison of one-photon (left) and two-photon (right) excitation of a denitrifying anaerobic granule at 0  $\mu\text{m}$  (top) and 41  $\mu\text{m}$  (bottom) depth. Staining was performed with the protein-specific fluorochrome SyproOrange. Note the improved signal and resolution in deep layers after two-photon excitation (bottom right). (d) Fluorescence lifetime imaging of autotrophic spherical biofilm microcolonies after staining with Syto13. Note the different lifetimes when individual bacteria in the microcolonies are compared. With permission of the American Society for Microbiology. See Walczysko *et al.*, 2008 for details. (e) *Pseudomonas* mixed-species flow cell biofilm showing two different strains labelled with GFP and dsRED. The two strains clearly develop into microcolonies of different structures. See Tolker-Nielsen *et al.* (2000) for details. (f) Dome-shaped, dual-species biofilm of *Pseudomonas* wild type (yellow) and mutant (blue) shown as XY and Z projections. The wild type forms caps on the stalks consisting of the mutant strain. See Klausen *et al.* (2003) for details. (e) and (f) are reproduced with the permission of Tim-Tolker Nielsen, the American Society for Microbiology and Blackwell Publishing.

the various fluorochromes can be found elsewhere (Haugland, 2005). A major component of bioaggregates and biofilms are EPS. The EPS produced by the microbial community include a variety of different biochemical polymers including polysaccharides, proteins, nucleic acids and amphiphilic compounds with different functionalities (Flemming *et al.*, 2007). Because of their complexity, the EPS are very challenging to analyse chemically, especially in environmental samples. Therefore, an *in situ* approach to analyse the glycoconjugate fraction of the EPS by means of fluorescence lectin-binding analysis has been suggested (Fig. 1a and b). In order to select

the appropriate lectin or a selection thereof, a lectin screening is necessary usually in combination with a nucleic acid counterstain (Neu & Lawrence, 1999; Neu *et al.*, 2001; Staudt *et al.*, 2003). By means of this *in situ* technique, an estimate of EPS-specific glycoconjugates can be made and even multiple types of glycoconjugates can be differentiated (Lawrence *et al.*, 2007b). Another way to record structural information is possible by fluor-labelled polymers, for example dextrans and fluorescent beads. Both compounds can be used to probe the shape and density of biofilm systems (Lawrence *et al.*, 1994).

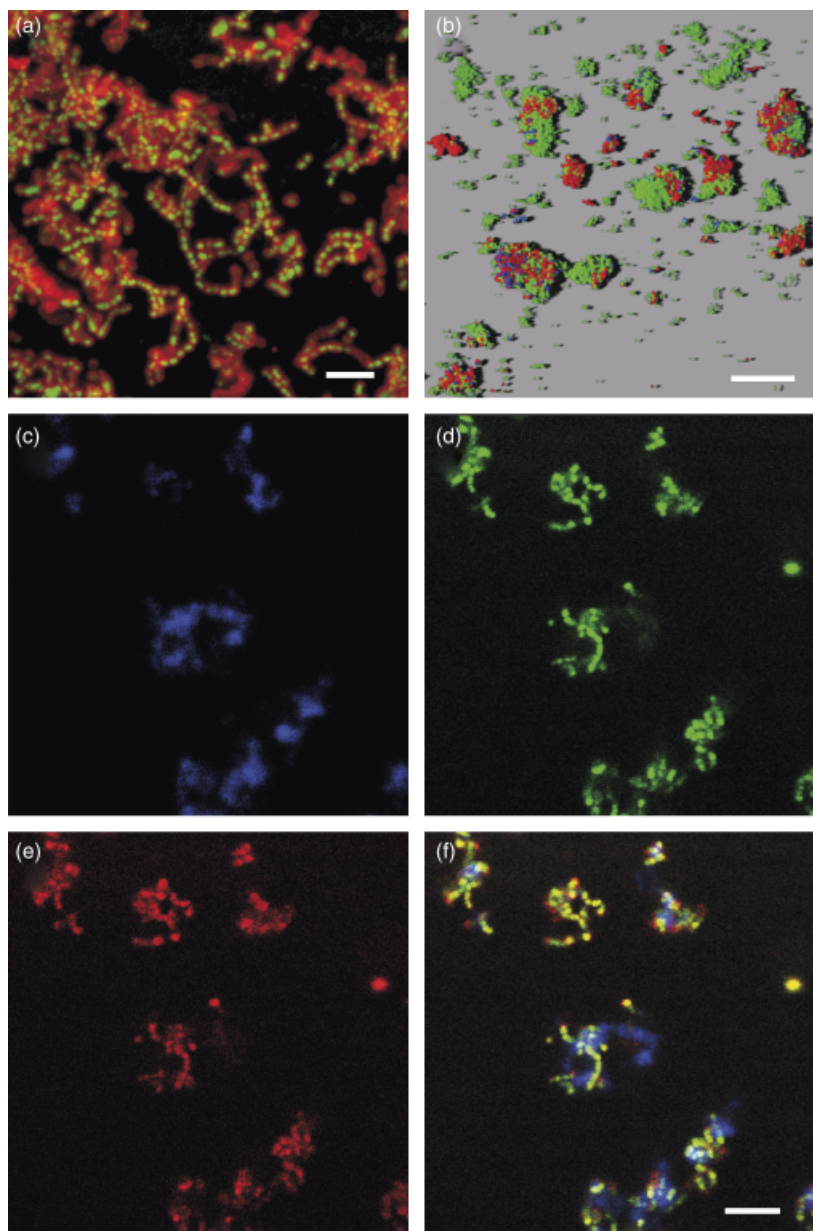


**Fig. 2.** LSM of immunostained oral bacteria. (a) Flow cell biofilm of *Streptococcus gordonii* after staining with Syto9 (= green) and a secondary antibody labelled with quantum dots (QD655 = red). Note the halos due to cell surface binding of antibody. Scale bar = 4  $\mu\text{m}$ . (b) SFP rendering of a triple primary immunostained *in vitro* biofilm containing *Veillonella atypica* (= blue), *S. gordonii* (= green) and receptor-polysaccharide-bearing *Streptococcus oralis* (= red). *Streptococcus oralis* binds to *S. gordonii* by recognition of receptor-polysaccharide. *Veillonella atypica* grows using lactic acid produced by streptococci. Scale bar = 30  $\mu\text{m}$ . (c–f) Triple channel image of *Streptococcus mutans* after staining with calcofluor white for glycoconjugates (blue = c), Syto9 for nucleic acids (green = d) and quantum dot (QD655) immunostained cell surfaces (red = e). In (f), the overlay of all three signals (c–e) is shown. Scale bar = 5  $\mu\text{m}$ . (a–f), image courtesy of Natalia Chalmers, Rob Palmer and Paul Kolenbrander, NIDCR/NIH, USA.

### Identification of community members

A second main LSM application is imaging of FISH using rRNA-targeted oligonucleotide probes (Ward, 1989; Amann *et al.*, 1995; Alfreider *et al.*, 1996; Moter & Göbel, 2000). Traditionally, epifluorescence microscopy was used for FISH analysis. However, due to multiple probe applications, the study of microbial interactions and the need for spatial information LSM became the method of choice. In the meantime, the original OLIGO-FISH technique evolved into many improved versions (Wagner *et al.*, 2003; Schmid *et al.*, 2006). Especially, CARD-FISH, which has improved

sensitivity, and FISH-MAR, which simultaneously reveals the identity and activity, are now frequently used (see Table 3 for details and references). Examples are given for CARD-FISH (Fig. 3a) and FISH-MAR (Fig. 3b–e).

### Immunofluorescence detection

Selective detection of bacteria using specific antibodies has been applied for a long time usually in combination with electron or epifluorescence microscopy. The immunofluorescence analysis of environmental biofilm samples by means of LSM was initially performed in studies of bacteria–plant

**Table 3.** Overview on fluorescence *in situ* hybridization and isotope imaging techniques as well as their combination

FISH-technique	Application	References
OLIGO-FISH (oligonucleotide-FISH)	Numerous examples	Ward (1989), Saylor & Layton (1990), Amann <i>et al.</i> (1995), Alfreider <i>et al.</i> (1996), Moter & Göbel (2000)
POLY-FISH (polynucleotide-FISH)	Marine plankton	DeLong <i>et al.</i> (1999), Wagner <i>et al.</i> (2003)
RING-FISH (recognition of individual genes-FISH)	Denitrifiers, activated sludge	Zwirgelmair <i>et al.</i> (2003a, b), Pratscher <i>et al.</i> (2009)
PNA-FISH (peptide nucleic acid-FISH)	Marine cyanobacteria, <i>Brettanomyces</i> , mycobacterium	Worden <i>et al.</i> (2000), Perry-O'Keefe <i>et al.</i> (2001), Stender <i>et al.</i> (2001), Wagner <i>et al.</i> (2003), Lehtola <i>et al.</i> (2006)
LNA-FISH (locked nucleic acid-FISH)	Yeast, bacterial pure cultures	Thomsen <i>et al.</i> (2005), Kubota <i>et al.</i> (2006)
CLONE-FISH (16S rRNA gene clone-FISH)	Bacterial pure cultures, bacterioplankton	Schramm <i>et al.</i> (2002), Wagner <i>et al.</i> (2003)
CARD-FISH (catalysed reporter deposition-FISH)	Pure cultures, activated sludge, cyanobacteria, picoplankton, marine bacteria, freshwater picoplankton, soil bacteria, marine epiphytic bacteria, symbiotic marine bacteria	Schönhuber <i>et al.</i> (1997), Schönhuber <i>et al.</i> (1999), Not <i>et al.</i> (2002), Pernthaler <i>et al.</i> (2002), Sekar <i>et al.</i> (2003), Blazejak <i>et al.</i> (2005), Ferrari <i>et al.</i> (2006), Tujula <i>et al.</i> (2006)
MAR-FISH (microautoradiography-FISH)	Defined mixed cultures, activated sludge, <i>Achromatium</i> , <i>Thiotrix</i> , <i>Nitrospira</i> , iron reducers, sulphate-reducing bacteria, nitrifying biofilms, marine bacterioplankton	Lee <i>et al.</i> (1999), Gray <i>et al.</i> (2000), Nielsen <i>et al.</i> (2003), Okabe <i>et al.</i> (2005), Sintes & Herndl (2006)
FISH-SIMS (first fluorescence <i>in situ</i> hybridization-SIMS)	Archaea-bacteria consortium from methane-rich marine sediments	Orphan <i>et al.</i> (2001)
RAMAN-FISH stable-isotope Raman spectroscopy-FISH	Reference cultures	Huang <i>et al.</i> (2007)
EL-FISH/nanoSIMS (element labelling-FISH/nanoSIMS)	<i>E. coli/V. cholerae</i> cultures, microbial consortium ( <i>Anabaena/Rhizobium</i> ), sample from human gingival sulcus	Behrens <i>et al.</i> (2008)
NanoSIMS/CARD-FISH (naniSIMS-catalysed reporter deposition-FISH)	Sulphur cycling at oxycline in a hypersaline microbial mat	Fike <i>et al.</i> (2008)
SIMSISH (SIMS- <i>in situ</i> hybridization)	Different <i>E. coli</i> cultures	Li <i>et al.</i> (2008)
HISH-SIMS (halogen <i>in situ</i> hybridization-SIMS)	Anaerobic phototrophic bacteria at the chemocline of an oligotrophic, meromictic lake	Musat <i>et al.</i> (2008)

The table explains the acronyms, indicates their application and gives selected references.

interactions (Schloter *et al.*, 1993; Assmus *et al.*, 1997; Schloter *et al.*, 1997; Gilbert *et al.*, 1998). Other reports have been published investigating nitrifying bacteria (Bartosch *et al.*, 1999), ammonium-oxidizing bacteria (Pinck *et al.*, 2001) or bacteria in oral biofilms (Gu *et al.*, 2005). Compared with epifluorescence microscopy, the main advantage of laser microscopy was the possibility of multichannel recording of three-dimensional data sets and the improved control of autofluorescence. In the meantime, the technique with fluorochrome-labelled antibodies and LSM analysis found its way into the manuals of microbial ecology and environmental microbiology (Schmid *et al.*, 2004, 2006; Dazzo *et al.*, 2007). The development of high-efficiency, long-lived Q-dot fluorophores as labels for nonfluorescent proteins has led to their use as a marker for antibodies targeting the bacterial cell surface. This approach was examined in detail using human oral bacteria in a suspension as well as in the form of biofilms (Chalmers *et al.*, 2007). Examples for immunostaining using Q-dots are presented in Fig. 2a–f.

## Reporter gene techniques

Fluorescent reporter genes represent a valuable tool to study microbial communities as this approach does not require staining of the sample (Leveau & Lindow, 2002; Janssen, 2003). The green fluorescent protein (GFP) as a cell marker for ecological and environmental studies has been proved to be especially useful (Errampalli *et al.*, 1999; Larrainzar *et al.*, 2005). GFP may also be used in order to investigate protein location within bacterial cells (Phillips, 2001). The applicability of various GFP types having different excitation and emission characteristics for specific labelling of different bacterial strains has been discussed (Christensen *et al.*, 1999). By combining GFP labelling of bacteria and LSM examination of the communities, major progress in the structure–function of microbial biofilm systems has been achieved. A whole series of publications by the group of Sören Molin demonstrates how GFP can be used to study microbial interactions in defined mixed cultures developed in laboratory microcosms (see e.g. Molin & Givskov, 1999). An example of GFP- and

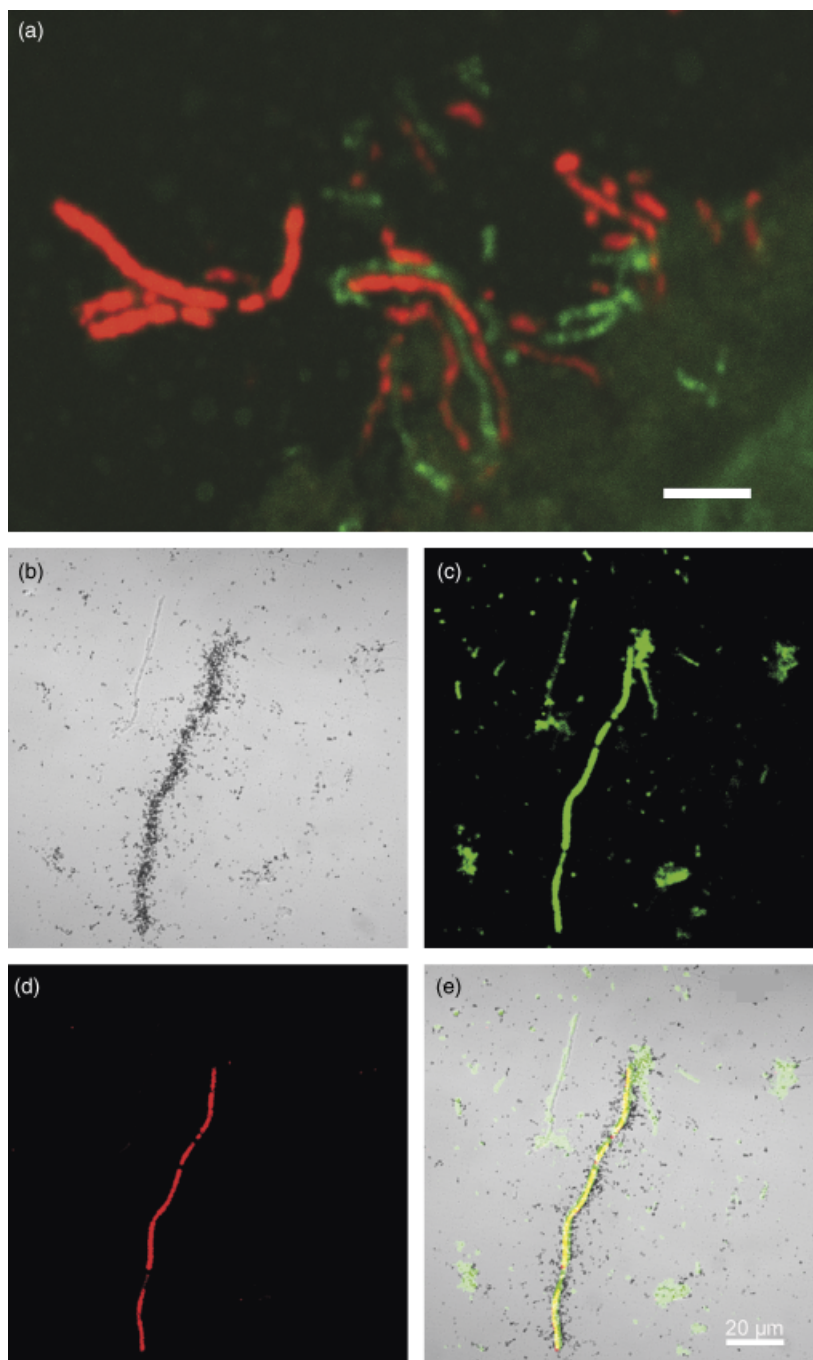


**Fig. 3.** LSM using fluorescence molecular biology techniques and activity measurements applied to microbial communities. (a) CARD-FISH of a microbial community from the gut of a marine oligochaete double-stained with Gamma-HRP-Alexa633 (= red) and Epsilon-HRP-Alexa488 (= green). Scale bar = 5 µm. Image courtesy of Caroline Ruehland and Nicole Dublier, MPI for Marine Microbiology, Bremen, Germany. (b–e) MAR-FISH example showing the uptake of  $^{14}\text{C}$ -labelled propionate by filamentous *Alphaproteobacteria*. The series demonstrates in (b) the black silver grains from MAR, in (c) the EUBmix probe in green, in (d) the ALF968 probe in red and in (e) the resulting overlay. Images courtesy of Per Halkjer Nielsen, University of Aalborg, Denmark.

dsRED-labelled *Pseudomonas* strains developing into a mixed biofilm is given in Fig. 1e. Another example shows the interaction of two *Pseudomonas* strains that were differentially labelled with CFP and YFP (Fig. 1f).

### Two-photon laser scanning microscopy

CLSM has some limitations that may be overcome by two-photon LSM. Excitation with two photons of half the energy

(usually infrared) allows a deeper penetration into light-scattering samples. Because of the longer wave length, two-photon imaging has an improved resolution in deeper sample locations. Another advantage is that the two-photon effect occurs only in the focal plane, thereby protecting out-of-focus areas from bleaching (Neu & Lawrence, 2005). The first paper on two-photon imaging showed the advantages of the technique in microbiology using densely grown oral biofilms (Vroom *et al.*, 1999). The technique was also used

to study stromatolites by combining one-photon and two-photon imaging of the microbial community and the associated mineral constituents (Decho & Kawaguchi, 1999; Kawaguchi & Decho, 2002). In a screening of various fluorochromes used in microbiology, their excitation characteristics for two-photon LSM were examined (Neu *et al.*, 2002). Because of the strong autofluorescence signal of chlorophyll *a* and phycobilin pigments, two-photon LSM can be easily applied for examination of phototrophic biofilms (Neu *et al.*, 2004b). The general suitability of two-photon LSM in microbial ecology has been discussed recently (Neu *et al.*, 2004a). The improved resolution of two-photon LSM in deep biofilm regions was used to study thick *Escherichia coli* biofilms and the spatial distribution of zinc (Hu *et al.*, 2005). Despite the advantages of two-photon LSM, only a few applications in the microbiological field were reported. From this, it may be concluded that the workhorse in laser microscopy of microbiological samples is still CLSM with one-photon excitation. See Fig. 1c for a comparison of one-photon vs. two-photon imaging.

### Lifetime imaging

An excited fluorochrome carries two pieces of information: firstly, the intensity, and secondly, the lifetime. The latter is a rather neglected parameter, which, however, may contain valuable additional information regarding the sample. The lifetime of a fluorochrome may occur as fluorescence or as luminescence (Clegg *et al.*, 2003; Gerritsen *et al.*, 2006). For example, variations in the fluorescence lifetime of carboxyfluorescein have been used to measure the pH in dental biofilms (Vroom *et al.*, 1999). Another application is the differential lifetime of the nucleic acid-specific fluorochrome Syto 13 when bound to DNA or RNA (van Zandvoort *et al.*, 2002; Neu *et al.*, 2004a; Walczysko *et al.*, 2008). It could be shown that Syto 13 may be used as a probe to measure the presence of single- or double-stranded nucleic acids (Fig. 1d). Fluorochromes with a delayed emission may be used in the luminescence lifetime imaging of, for example oxygen at the macroscopic scale (Holst & Grunwald, 2000; Liebsch *et al.*, 2000). Very recently, this approach was applied at the microscopic scale in order to study the oxygen distributions in microcolonies developed in flow-through cells (Kühl *et al.*, 2007).

### Future LSM applications

In order to complete the section on LSM, several new approaches, for example 4pi, STED, photoactivation localization microscopy and stochastic optical reconstruction microscopy (PALM/STORM) and structured illumination microscopy (SIM), are briefly mentioned as these LSM techniques are now commercially available. One of the limitations of LSM is the unequal resolution in *XY* and *Z*. This can be circumvented by increasing the numerical

aperture (NA) of the objective lens. By using two opposed lenses and mounting the sample between two coverslips, equally resolved *XYZ* data sets may be recorded from fixed or living samples (Schrader *et al.*, 1998; Bahlmann *et al.*, 2001). A first application using the 4pi commercial instrument describes the structure of chromatin (Bewersdorf *et al.*, 2006). STED represents a technique that overcomes the diffraction barrier and therefore has a higher resolution as compared with conventional LSM. STED, however, requires specific fluorochromes that can be excited and depleted (Klar *et al.*, 2000; Donnert *et al.*, 2006). In the meantime, two other high-resolution techniques based on stochastic switching and readout are becoming available. PALM and STORM take advantage of a similar approach. The proof of principle was already demonstrated in 2006 (Hess *et al.*, 2006; Rust *et al.*, 2006). In the meantime, several cell biology applications have been published (Bates *et al.*, 2007; Shroff *et al.*, 2007; Huang *et al.*, 2008a, b; Shroff *et al.*, 2008). In fact, PALM in the total internal reflection fluorescence (TIRF) mode was already used to study the distribution of cell surface proteins in *E. coli* (Greenfield *et al.*, 2009). SIM represents another high resolution technique and takes advantage of the so-called Moire effect. By using a structured light pattern for excitation, normally inaccessible high-resolution information becomes visible. As a result, twice the resolution of conventional laser microscopy can be achieved (Gustafsson, 2000; Shermelleh *et al.*, 2008). Very recently, the new concepts of high-resolution imaging have been compared and discussed; all of them are pushing the resolution of laser microscopy across the diffraction barrier postulated by Abbe more than 100 years ago (Hell, 2007, 2009). In contrast to high-resolution techniques, but at a larger scale, optical coherence tomography (OCT) can be used to examine extended sample areas in the millimetre range. Based on scattering properties, OCT allows imaging of microbial biofilms without adding probes or fluorochromes (Xi *et al.*, 2006; Haisch & Niessner, 2007).

For those further interested in LSM, several extensive reviews have been published, all of which have a different focus. The initial reviews provided a general overview of the LSM imaging approach in microbiology (Lawrence *et al.*, 1998; Lawrence & Neu, 1999), discussed technical and practical aspects of LSM (Lawrence & Neu, 2007b; Lawrence *et al.*, 2007a) and suggested a structured approach of how to analyse an unknown microbiological sample (Neu & Lawrence, 2002). The more recent reviews concentrated on the applicability of one-photon and two-photon LSM for the analysis of microbial communities (Neu & Lawrence, 2005), imaging of biopolymer distribution (Lawrence *et al.*, 2005), spatiotemporal LSM approaches including different molecular techniques (Palmer *et al.*, 2006) and the application of CLSM for studying flocs and particles (Lawrence & Neu, 2007a).

## MRI

### MRI basics

The phenomenon of NMR describes the absorption of electromagnetic energy by atomic nuclei in an external magnetic field. It relies on the quantum mechanical effect that many nuclei carry a spin and therefore a magnetic moment. When such a sample is exposed to a strong, homogeneous, polarizing magnetic field, a small magnetization along this field is induced inside the sample. The orientation of this magnetization can be manipulated by irradiating the sample with an isotope-specific resonance frequency, the so-called Larmor frequency, which is directly proportional to the strength of the polarizing field. Upon return to thermal equilibrium, a process called relaxation, the stored energy is released again, giving rise to a small, but measurable magnetic resonance signal. Slight magnetic field variations due to the electrons orbiting the nuclei lead to a shift in the energy level, and therefore the resonance signal, which is characteristic for the chemical bond of the given nucleus. This so-called chemical shift allows the chemical analysis and structure determination of large molecules.

Although in principle any nucleus of nonzero nuclear spin can be studied with magnetic resonance, the  $^1\text{H}$  nucleus (proton) is the most commonly used nucleus due to its high natural abundance and high MR sensitivity. Because the energies of these transitions are low compared with the energy of the thermal fluctuations, the populations in the excited and nonexcited state differ only by a small amount. Therefore, NMR is considered a relatively insensitive method compared with optical methods. However, as a consequence of these low energies, no ionizing radiation is involved, which is a huge advantage when studying living objects (Rinck, 2001; McRobbie *et al.*, 2006).

### The MRI method

NMR imaging is based on the fact that the Larmor frequency is proportional to the polarizing magnetic field. If in addition to the external magnetic field a uniform magnetic field gradient is applied, this frequency becomes spatially dependent, which provides a means to measure two- and three-dimensional images of the spin distribution (Mansfield & Morris, 1982; Callaghan, 1991). In practice, these magnetic field gradients are created by passing large, switchable currents through specially designed gradient coils, which are placed around the sample.

As stated above, each measurement disturbs the magnetization from its thermal equilibrium. The way in which the magnetization returns to the ground state is known as relaxation. There are two basic processes of relaxation: spin–lattice relaxation, which involves an exchange of energy between the spins and the surrounding thermal reservoir

(lattice), and spin–spin relaxation, in which spins come to a thermal equilibrium among themselves. The corresponding relaxation times are referred to as  $T_1$  and  $T_2$ , respectively. These relaxation times are mainly governed by the rotational and translational freedom of the corresponding molecules and the amount of paramagnetic impurities, such as salts or dissolved oxygen. Generally, both  $T_1$  and  $T_2$  are shortened by reducing the molecular mobility and by a higher amount of paramagnetic ions, for example  $\text{Co}^{2+}$ ,  $\text{Cu}^{2+}$ ,  $\text{Mn}^{2+}$ ,  $\text{Gd}^{3+}$ . A relaxation time map is an image where each pixel (voxel) value corresponds to the relaxation time at the pixel (voxel) location. This information is complementary to the proton density and has been used to characterize biofilm structures (Abragam, 1961; Slichter, 1990).

Displacements of molecules can be measured using the pulsed gradient spin echo NMR method (Stejskal & Tanner, 1965). Similar to the case of imaging, the method uses magnetic field gradients, but in a sort of ‘difference mode’. The molecules are encoded for position by one gradient pulse. After a well-defined delay time, a second pulse is applied to reverse the encoded position. If the molecules have moved along the direction of the applied gradient, a phase shift in the signal remains, which is proportional to the distance the molecules have travelled over this delay time. For uncorrelated, Brownian motion of many molecules, the amplitude of the echo signal decreases due to molecular self-diffusion. By measuring the NMR signal with increasing gradient strength, flow velocities as well as self-diffusion and dispersion coefficients can be determined (Callaghan, 1991; Callaghan & Xia, 1991; Manz & Callaghan, 1997; Manz *et al.*, 1998, 1999a, b, 2003; Seymour *et al.*, 1999; Manz, 2004).

### MR measurements of transport properties in biofilms

NMR measurements provide an easy and noninvasive way to study the transport properties in biofilm systems. The hydrodynamic properties of the boundary layer between the biofilm and the bulk phase (interface between both) govern the interaction of the biofilm matrix with the bulk phase. The nutrients need to be transferred from the bulk phase through the boundary layer to the biofilm. The mass transfer of a stagnant fluid into the pore network of the porous biosystem can be described by an effective diffusivity, which is defined by Fick’s first law (Horn, 2003). Such a purely diffusive transport between biofilm and bulk driven by concentration gradients would result in a linear concentration profile through the boundary layer. Any additional convective mass transfer would result in a nonlinear concentration profile through the boundary layer. Therefore, there is a strong interest in the direct and noninvasive measurement of transport processes in these systems and MRI on a microscale is well suited to address these issues.

In the first MR study of transport properties in biofilm systems, Lewandowski *et al.* (1993) measured the profiles of the flow velocity and dissolved oxygen concentration. The authors found that within the hydrodynamic boundary layer, both profiles can be described by exponential equations, confirming that both convective and diffusive transport occur through the boundary layer. In systems that consist of a combination of free, unrestricted water and water bound to a network of microorganisms (as is the case for biofilms), a diffusion-weighted NMR experiment can be used to discriminate between both populations and measure the proportion of biomass in the medium (Potter *et al.*, 1996) as well as the porosity (La Heij *et al.*, 1996; Potter *et al.*, 1996; Beuling *et al.*, 1998; van As & Lens, 2001; Lens & van As, 2003), allowing the user to characterize biomass inside a laboratory column or in flow cell experiments noninvasively and in real time. The effect of biofilm growth on the transport properties in flowing systems has been studied by Seymour *et al.* (2004a). In a clean-packed bed reactor, the uniform pore size distribution and permeability leads to a normal Gaussian displacement distribution of the flowing liquid. The biofilm growth induces a heterogeneous transition with variable pore size and blocked pores, which generates a non-Gaussian displacement distribution. This leads to a transition from normal to anomalous hydrodynamic dispersion as the biofilm grows in the reactor.

### Mapping biofilms using MRI

At first glance,  $^1\text{H}$ -MRI appears to be unsuitable to map the structure of biofilms in a wet environment due to the lack of contrast in the density of  $^1\text{H}$  nuclei between the biomass and the bulk phase, considering that most biofilms consist of more than 95% of water. This being true for proton density, NMR offers a wealth of parameters through which additional contrast can be applied to the images. For example, in biofilms, the mobility of the water is restricted by the EPS matrix and the microbial cells, whereas motion of the water in the bulk phase is unrestricted. Furthermore, the biofilm matrix accumulates minerals from the growth medium, leading to a contrast in the relaxation times between the biofilm and the bulk phase. Hoskins *et al.* (1999) were the first to exploit this contrast in order to selectively image biofilms in aqueous systems. They compared the relaxation time distributions of biofilm and bulk phase in an open-flow reactor with a porous system bioreactor made from packed glass beads. While in the open-flow reactor both the  $T_1$  and  $T_2$  distributions are bimodal with two distinct fluid phases (bulk and biofilm associated), this is only the case for the  $T_1$  distribution in the packed bead reactor. There, the components of the  $T_2$  distribution cannot be resolved, because the pore surface relaxation leads to an extra broadening of the  $T_2$  distribution. Accumulation of paramagnetic ions in the

biofilm reduces the relaxation time. This effect has been used to quantify and spatially resolve the  $\text{Co}^{2+}$  ion concentration in a biofilm-mediated ion exchanger (Graf von der Schulenburg *et al.*, 2008a).

While the biofilm can be resolved well via relaxation time contrast in stationary systems, a flow-weighted imaging technique is more suitable in flowing systems (Metzger *et al.*, 2006). With such an NMR pulse sequence, the biofilm accumulation in a packed bed reactor could be imaged continuously. The results indicated that the nonstationary flow through the biofilm reactor changes significantly due to the changing morphology, confirming previous spatially nonresolved NMR measurements (Seymour *et al.*, 2004a). The porosity value of 0.4 determined via NMR was in agreement with gravimetric measurements. More recently,  $^1\text{H}$  MRI was used to determine the diffusivity of copper in phototrophic biofilms. The technique is suggested as a tool for studying the fate of paramagnetic metals in natural microbial biofilms (Phoenix & Holmes, 2008).

### MRI measurements of structure/flow relationship

From the previous sections, it is clear that there is a mutual dependence between the biofilm structure and the flow field of the bulk phase. MRI is the method of choice to study this dependence, because it allows the noninvasive measurement of both properties in the original cultivation environment. Structural data for a biofilm surface in a tube reactor, along with velocity profiles of the bulk phase and within the hydrodynamic boundary layer, were first presented by Manz *et al.* (2003). At some locations on the biofilm surface, the local shear stress, which can be calculated from the velocity profiles, is significantly higher than the mean wall shear stress. In subsequent studies (Manz, 2004; Manz *et al.*, 2005), these regions of high shear stress are identified as the locations where detachment of biomass usually occurs when the flow rate is increased (forced detachment). See the example in Fig. 4.

Further studies on the impact of biofilm growth on the three-dimensional velocity field have been performed in capillary reactors (Seymour *et al.*, 2004b; Gjersing *et al.*, 2005) and in packed bed reactors (Nott *et al.*, 2005). The amount of stagnant water that is trapped in the biofilm matrix or blocked pores increases with biofilm growth and the flow field experiences significant changes through the development of secondary flow.  $^{13}\text{C}$  pulsed field gradient NMR has been applied in order to measure the mass transfer in biofilms associated with polyurethane foam. This technique will allow assessment of transport processes including nutrients, metabolic products, pollutants or biocides (Graf von der Schulenburg *et al.*, 2008b).

So far, MRI time-resolved studies have demonstrated the potential of the technique in order to study: mapping of

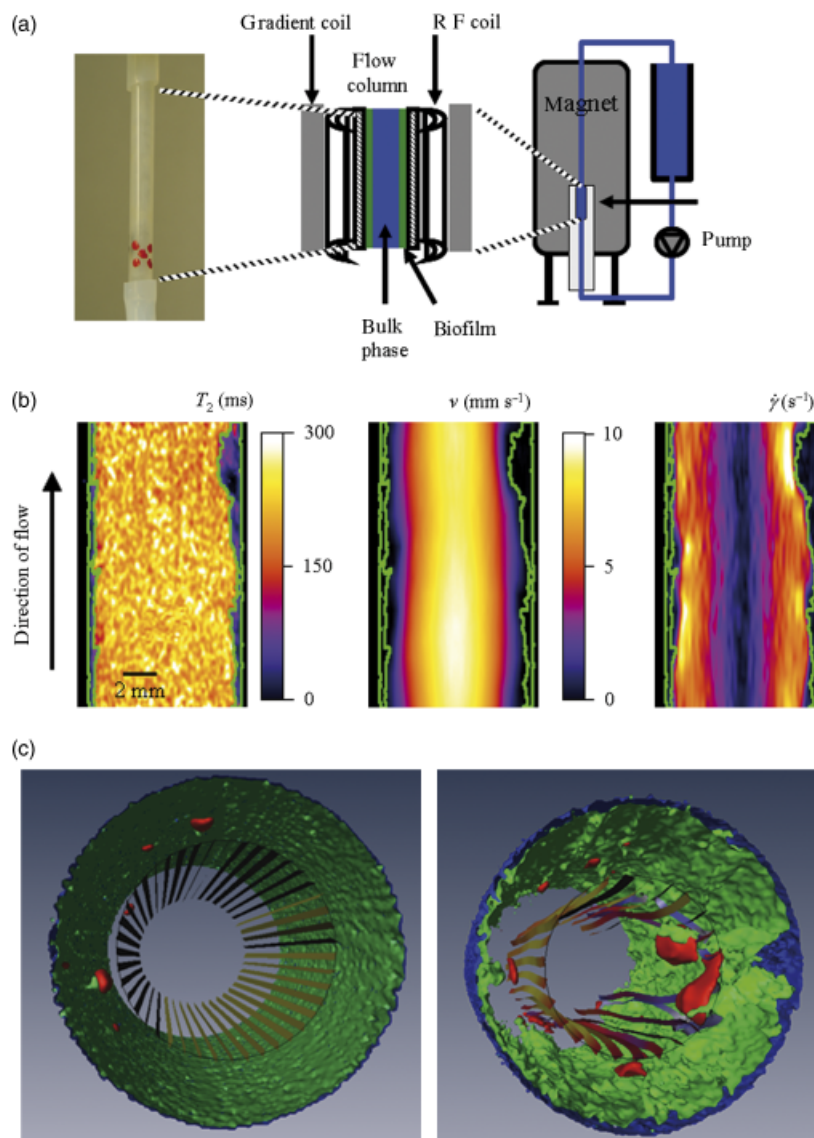


**Fig. 4.** (a) Set-up of the MR experiments for tube reactor biofilm samples. The test segment with the biofilm (left) is placed into the NMR probe with the radio frequency and gradient coils (middle). After connecting the flow loop through the bore of the magnet, the probe with sample is inserted into the magnet (right). (b) A set of parameter images is shown for one axial slice through the centre of a three-dimensional image of a biofilm sample. The  $T_2$  relaxation time is significantly reduced in the biofilm compared with the bulk liquid. This allows the determination of the biofilm structure (left). For the same slice, the axial flow velocities (middle) and shear rates (right) are shown, which yield information about the transport properties and forces acting on the biofilm surface. The biofilm surface, as obtained from the  $T_2$  image, is shown as a green line in all images. (c) A three-dimensional visualization of the inner tube surface (blue), biofilm structure (green surface), flow field (ribbons) and regions of high shear rate (red surface). The image on the left shows flow through a tube with a smooth surface. The flow field is mainly parabolic; only small biofilm filaments attached to the tube wall lead to slight distortions in the flow field, which also result in high shear rates in their vicinity. In a tube with a thick, rough biofilm, the flow profile is forced to be nonparabolic (right). The regions with a high shear rate are mostly located near large filaments penetrating the flow field.

structural biofilm features, flow and transport characteristics within microbial biofilms, flow velocity in immobilized microbial communities, biofilm structure/flow relationships, transport properties and diffusion in biofilms. Finally, there is one report on correlated biofilm imaging using NMR combined with confocal laser microscopy. For this investigation, the authors used a special instrument that allowed integration of both techniques (McLean *et al.*, 2008).

## STXM

### Imaging and spectroscopy

STXM uses near-edge X-ray absorption fine structure/spectroscopy (NEXAFS) as the contrast mechanism, whereby the collection of image sequences over a range of energies

provides detailed quantitative mapping of chemical species because the NEXAFS is based on the bonding structure of a particular chemical species (Kirz *et al.*, 1995; Ade & Urquhart, 2002; Ade & Hitchcock, 2008). A schematic of a typical X-ray STXM beamline (Bluhm *et al.*, 2005; Kaznatcheev *et al.*, 2007) and microscope (Kirz & Rarback, 1985; Kilcoyne *et al.*, 2003) is given in Fig. 5. STXM can be conducted using either soft or hard X-rays, with most elements having an absorption edge in both energy ranges. The soft X-ray energy ranges of the Molecular Environmental Sciences beamline at the Advanced Light Source (ALS) (75–2100 eV) and the spectromicroscopy beamline at the Canadian Light Source (CLS) (200–2600 eV) coincide with the K-edges of the major earth elements (C, N, O, Na, Mg, Al and Si), the L-edges of important transition metals (Ti, V, Cr, Mn, Fe, Co, Ni, Cu and Zn), the L-edges of P, S, Cl, K and

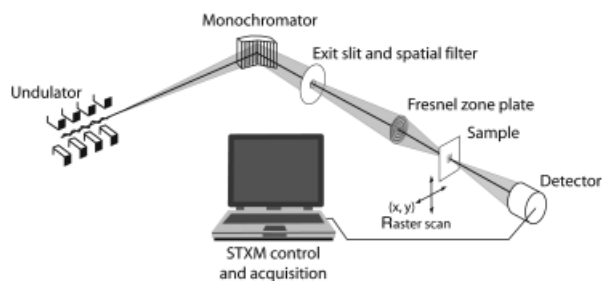


**Fig. 5.** Schematic of a STXM on an undulator beamline such as ALS 11.0.2 or CLS 10ID1. Synchrotron (not shown), undulator source, beamline, STXM enclosure and optics as well as acquisition.

Ca, and the K-edges of P and S (at CLS only). The power of the soft X-rays over hard X-rays is the ability to collect C, N and O information on biological and environmental samples, thus allowing for the quantitative mapping of organic species, including the major classes of biological macromolecules. Also, the spatial resolution of the soft X-ray is better than that of the hard X-ray, being about 30 vs. 150 nm. The fact that soft X-rays can penetrate water makes them ideal for studying hydrated samples. With the use of appropriate reference spectra, NEXAFS microscopy provides detailed, quantitative speciation and elemental analysis with part per thousand sensitivities for transmission detection (Jacobsen *et al.*, 2000). Because the method uses the intrinsic X-ray absorption properties of the sample, it eliminates the need for the addition of reflective, absorptive or fluorescent probes and markers that may introduce artefacts that complicate interpretation.

The first study to demonstrate the potential of soft X-rays for imaging bacteria examined early-stage *Pseudomonas putida* biofilms using a full-field transmission X-ray microscope with synchrotron radiation (Gilbert *et al.*, 1999). This study applied only a single photon energy, and so the analytical power of X-ray microscopy was not used. The power of soft X-ray NEXAFS microscopy for examination of microbial communities and biofilms has been demonstrated in a series of recent publications on mapping biomacromolecules (Lawrence *et al.*, 2003), metallic species ( $\text{Fe}^{2+}$ ,  $\text{Fe}^{3+}$ ,  $\text{Mn}^{2+}$ ,  $\text{Ni}^{2+}$ ) (Dynes *et al.*, 2006a) and the antimicrobial agent chlorhexidine (Dynes *et al.*, 2006b) in river biofilms. Bluhm *et al.* (2005) provide many examples of STXM applied to molecular environmental science including studies of biofilms and bacterial–mineral interactions.

### Sample preparation, data collection and analysis

In brief, dry biofilm samples and reference materials are deposited directly or as a wet slurry onto silicon nitride windows (Silson Ltd, UK, <http://www.silson.com/>, Norcada Ltd, Canada, <http://www.norcada.com/>) or after cryo-fixation and sectioning onto transmission electron microscope

(TEM) grids. Note that the chemical fixation of biofilms makes it impossible to collect meaningful data at the C K-edge. Biofilms may also be grown directly on the windows using the method of Lawrence *et al.* (2003) or transferred to a window after gentle removal from the substratum. Wet biofilm samples can be prepared by sealing the sample in between two silicon nitride windows (wet cell). In this case, the chamber is purged with helium instead of vacuum evacuated to prevent breakage of the wet cell.

Typically, 10–150 images over a range of energies (i.e. image sequence) are collected for a particular absorption edge for the biofilm and areas devoid of biofilm. The reason for collecting image sequences in the areas devoid of biofilm is to correct for the absorbance of the beam by the windows and the water. It is also important to assess the sample for damage, for example an image recorded at 289 eV will visualize radiation damage to polysaccharides in microbial samples (Dynes *et al.*, 2006a). In addition it is necessary to calibrate the microscope energy scale using sharp gas phase signals, most often the Rydberg peaks of  $\text{CO}_2$ .

Quantitative maps of the component of interest (e.g. protein, lipid, polysaccharide), can be derived from the image sequences by spectral fitting using linear regression procedures such as the singular value decomposition and stack fit (Jacobsen *et al.*, 2000; Dynes *et al.*, 2006a, b). Details of the fitting, difference analyses and mapping can be found in Dynes *et al.* (2006a, b). Reference spectra may be available in the literature or obtained through analyses of pure substances. Image and spectral processing may be performed with routines available from the National Synchrotron Light Source (NSLS) web site (Jacobsen, 2006) or by the AXIS2000 software (Hitchcock, 2008). Multivariate statistical analysis procedures are becoming increasingly powerful for analysing STXM image sequence data without preassumptions of the components present in the sample (Jacobsen *et al.*, 2003; Lerotic *et al.*, 2004, 2005).

### Synchrotron facilities

Soft X-ray imaging and spectromicroscopy may be carried out at a number of facilities worldwide including the National Synchrotron Light Source (NSLS), the Advanced Light Source (ALS), the Canadian Light Source (CLS), Elettra (Italy) and the Swiss Light Source (SLS). Soft X-ray STXMs are under construction at the Stanford Synchrotron Light Source (SSRL), the Berlin synchrotron (Bessy), the Shanghai source (SSRF), French synchrotron (Soleil) and the Spanish synchrotron (Alba). Tender X-rays (2–8 keV) are available at each of the three third-generation high-energy rings: European Synchrotron Facility (ESRF), Argonne Advanced Photon Source (APS) and SP ring-8 in Japan. Most of our studies to date have been carried out at the ALS (Berkeley, CA) using the STXM microscopes at beamline 5.3.2 or 11.0.2 (Warwick *et al.*, 2002; Kilcoyne

*et al.*, 2003). Bluhm *et al.* (2005) discuss the set-up and properties of the Molecular Environmental Sciences beam-line (ALS 11.0.2) and its dedicated end-stations.

### Mapping metal species and organic contaminants

To date, the most extensive application of synchrotron radiation in combination with soft X-ray STXM has been for mapping of metals (Kemner *et al.*, 2004). Yoon *et al.* (2004) applied STXM to image interactions between *Caulobacter crescentus* and aluminium-containing nanoparticles. Images obtained using the C 1s and Al 1s edges revealed that the biochemistry of bacteria and the chemistry of the particles were closely associated in aggregates. STXM images showed rod-shaped bacteria associated with corundum and montmorillonite particles and they suggest that the association is via EPS produced by the bacteria. Chan *et al.* (2004) used STXM to show that microbially generated iron-oxhydroxide filaments contain polysaccharides. In this case, they concluded that the polysaccharide acted as a template for the formation of the metal oxide. Another aspect of STXM is the capacity to assess the oxidation state of the metal and the ligand form and identity. For example, Pecher *et al.* (2003) used STXM at the Mn 2p edge to differentiate Mn oxidation states in Mn nodules formed by spores of a marine *Bacillus*-SG1. They determined the relative amounts of Mn(II), Mn(III) and Mn(IV) in the spores and found that the more oxidized species were located outside of the cell membrane. Similarly, Toner *et al.* (2005) applied STXM at the Mn 2p edge to measure the conversion of Mn<sup>2+</sup> to Mn<sup>3+</sup> and Mn<sup>4+</sup> by *P. putida* strain MnB1. The *P. putida* removed Mn from solution and concentrated it as Mn(III) and Mn(IV) immediately adjacent to the bacterial cells. These Mn precipitates were completely enveloped by bacterial biofilm material. Benzerara *et al.* (2004) showed that *C. crescentus* cells, in the presence of a high calcium concentration, precipitated carbonate hydroxyapatite. Using STXM, they were able to simultaneously map the proteins, polysaccharides and nucleic acids at the single-cell scale. Benzerara *et al.* (2005) applied STXM to examine metal–microorganism associations in bioweathering products on a meteoritic Fe–Mg-orthopyroxene showing an amorphous Al-rich layer beneath the microorganism, calcium carbonates of unique morphology closely associated with polysaccharides adjacent to the microorganism and regions surrounding the microorganism with different iron oxidation states. Their results confirmed the existence of fine-scale environmental gradients surrounding bacteria cells on mineral surfaces. STXM is a promising tool for advancing the study of hydrated interfaces between minerals and bacteria, particularly in cases such as biofilms, where maintenance of a hydrated state is critical to the analyses.

Dynes *et al.* (2006a) report on the use of C 1s STXM to examine the spatial distribution of chlorhexidine (1,1'-hexamethylenedis[5-(*p*-chlorophenyl) biguanide]), a widely used antimicrobial agent, in river biofilm communities grown for 6 weeks in the presence of 100 µg L<sup>-1</sup> (100 p.p.b.) of chlorhexidine digluconate. STXM measurements allowed the authors to quantitatively map chlorhexidine, protein, lipids, polysaccharides, Ca<sup>2+</sup>, K<sup>+</sup>, CO<sub>3</sub><sup>2-</sup> and silica (SiO<sub>2</sub>) in two diatom species and a bacterial colony in the biofilm. STXM has moved rapidly from initial proof-of-concept studies imaging bacterial cells to detailed analysis of the biochemical composition of bacterial biofilms in combination with quantitative analysis of metals including speciation as well as mapping of organic compounds in the context of the biofilm.

### Mapping biomolecules

The C 1s NEXAFS region provides an excellent contrast and is probably the best to map the major biological macromolecules as well as the carbonate anion. Reference spectra for the major biomolecules, nucleic acids, protein, lipids and polysaccharides, as well as CO<sub>3</sub><sup>2-</sup> and K<sup>+</sup> are shown in Fig. 5 (Lawrence *et al.*, 2003; Chan *et al.*, 2004; Vyalikh *et al.*, 2005). The result from the spectral fitting of a C 1s image sequence collected from a region of a microbial biofilm is also shown in Fig. 6. In this case, the protein, lipid and saccharide signals have been localized and the colour composite map shows their distribution in a bacterial microcolony in combination with the CO<sub>3</sub><sup>2-</sup> and K<sup>+</sup> signal. Lawrence *et al.* (2003) found that STXM could be used effectively to map the spatial distributions of these major biomolecules in complex microbial biofilms. In that work, STXM and LSM imaging were applied to exactly the same location in a biofilm. This allowed assessment of the results of probe-dependent LSM relative to the absorbance spectra-based STXM. In general, the authors reported a reasonable agreement between the two methods. Benzerara *et al.* (2006) used NEXAFS spectra at the C and N K-edges to provide unique signatures for microorganisms in modern calcareous microbialites from the alkaline Lake Van, Turkey, at the nanometre scale. The results they obtained provided bio-signatures for these deposits and indicated a significant role for microorganisms in the formation of these structures.

### Final comments and conclusions

The successful analysis of microbiological samples with these advanced imaging techniques requires a number of considerations regarding the size and shape, preparation and mounting, necessity for probes as well as the resolution and electromagnetic energy necessary for imaging and analysis (Table 1). Ideally, the sample should be examined *in situ* in the fully hydrated state. This means that the fresh,

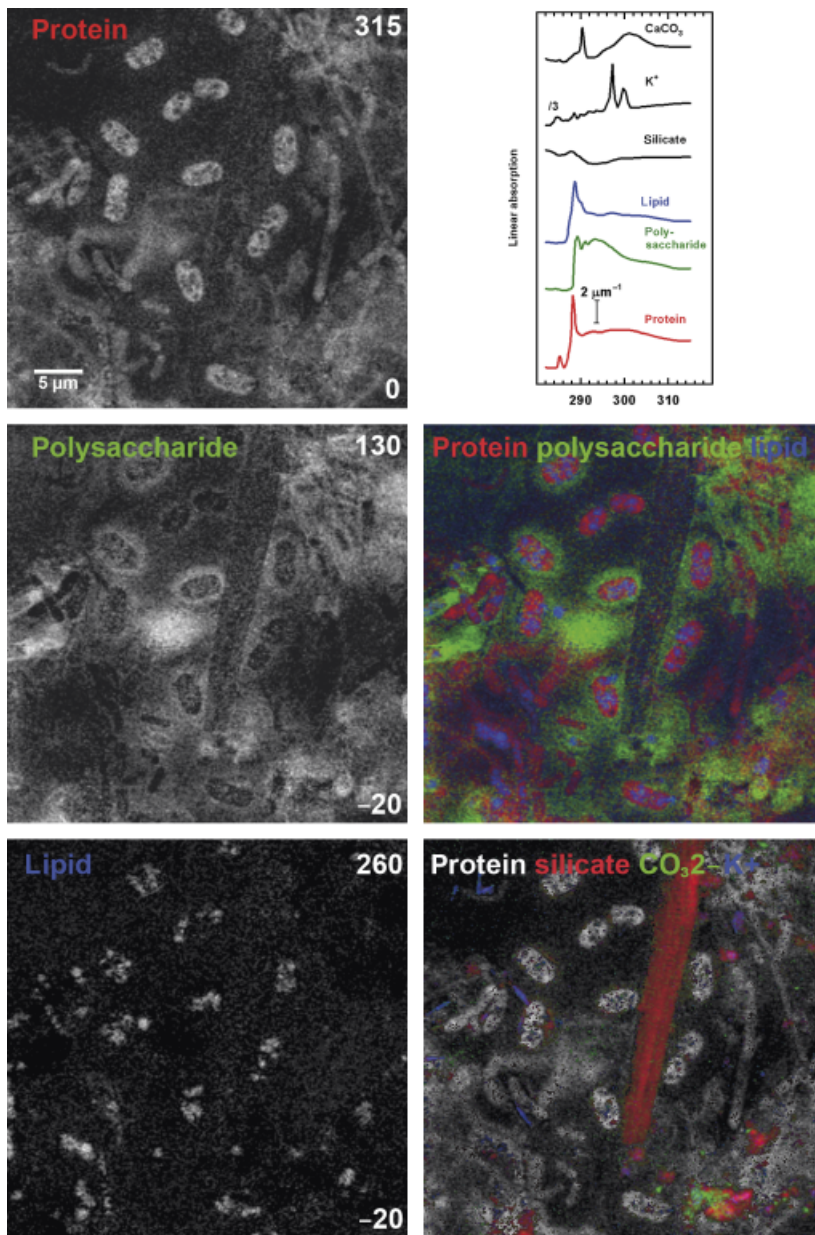


**Fig. 6.** Top right: C 1s NEXAFS spectra for the major biomolecules: protein, lipid, polysaccharides, as well as the signals from nonorganic species (the residual structure is from incomplete correction of the shape of the incident flux and represents silicate in this case),  $\text{CO}_3^{2-}$  and  $\text{K}^+$  (2p); note that the  $\text{K}^+$  spectra have been divided by 3. The vertical scale bar is on a quantitative linear absorbance scale. Left column: Grey-scale maps of the protein, polysaccharide and lipid signals from a river biofilm (Hitchcock *et al.*, 2005). The grey scales indicate thickness in nanometres. Right column: Three-colour overlay of the protein, lipid and polysaccharide maps (middle) and three-colour overlay of the no-carbon (mainly silicate), carbonate and potassium ion, superimposed on a grey-scale map of the protein (bottom).

living sample is directly used for imaging without chemical fixation. LSM and MRI fully match this necessity. In LSM with an upright microscope, the water immersible (dipping) lenses proved to be ideal for imaging microbial communities. For STXM, a wet mount can be examined, and with care, these windows can be used directly in controlled medium bioreactors, such that the sample examined is minimally disturbed from its growth environment.

The next issue is restrictions in terms of sample size and mounting. LSM and MRI analysis only have restrictions in terms of the geometry (cm) of either the objective lens – microscope stage dimension (LSM) or the diameter of the

sample port (MRI). For STXM imaging, the sample has to be very thin and a wet preparation must be mounted in between two fragile silicon nitride windows, each having a thickness of about 75 nm. This means a sample of 100–300 nm of organic dry matter for C 1s studies; much thicker samples (2–10  $\mu\text{m}$ ) can be used as long as they have an equivalent dry matter thickness. Recently, much more robust polyimide windows have been used successfully for STXM studies of wet biofilms (A.P. Hitchcock & M. Obst, pers. commun.).

Another important point is the necessity of stains, fluorochromes and other probes. LSM can take advantage of the

intrinsic sample properties including reflection and autofluorescence. The photosynthetic pigments of algae and cyanobacteria are especially useful markers for differentiation of the two groups (Neu *et al.*, 2004b). If microorganisms can be labelled by reporter gene technology such as GFP or variations thereof, staining is not necessary. Nevertheless, in many cases, fluorochromes or fluor-conjugated probes have to be applied for imaging of specific constituents and structures. This, of course, is a disadvantage as it may have an effect on the vitality of microorganisms. The advantage of both MRI and STXM is that they do not require the addition of probes for imaging. However, some probe-like compounds may be added in order to improve contrast or to locate specific features.

A further issue is the resolution at which the samples can be imaged and analysed. The resolution of LSM is dependent on the wavelength of laser light used ranging from UV to IR, the NA of the objective lens and the refractive index of the medium. As a result, the resolution in practice of biological samples showing absorption and scattering is at best in the range of 200–300 nm. Very recently, new commercial laser microscopy instruments using so-called nanoscopy (e.g. STED, PALM, STORM) are increasing the resolution of fluorescence techniques towards 20 nm (Hell, 2007, 2009). The resolution of MRI is dependent on the probes used and the optimization of pulse sequences. With state-of-the-art instruments, a resolution of approximately 5000 nm can be achieved. STXM intrinsically has a higher resolution as soft X-rays are used for imaging. Therefore, the state-of-the-art zone plate resolution is 15 nm (Chao *et al.*, 2005) and objects smaller than 30 nm are resolved routinely.

In conclusion, LSM represents one of the most versatile tools for studying microbial biofilm systems. Its popularity is based on the current broad availability of LSM instruments, the flexibility in terms of sample mounting and staining as well as the option for quantitative analysis of digital data. MRI is not as readily available and requires more instrumental experience for measuring microbial samples and subsequent data analysis. The advantage of MRI lies in the bulk analysis of the biofilm and the water phase in combination with information on hydrodynamic parameters in flowing systems. STXM is dependant on access to a synchrotron with the appropriate beamline and microscope. All of the soft X-ray microscopes are in high demand and access is controlled by a peer-review process of proposals, although there is no fee for noncommercial use. Sample size is a clear limitation; however, if it comes to the simultaneous analysis of organic and inorganic compounds at the microbial cell level, STXM allows chemical speciation and quantification that is not available with LSM or MRI. Each of the techniques has its dis/advantages and in-depth analysis of microbiological samples will require correlative imaging approaches. This combination has already been

shown for LSM/MRI (Manz *et al.*, 2006) and for LSM/STXM (Lawrence *et al.*, 2003).

A new and exciting development based on high-resolution (33 nm) imaging of isotopes will push the analysis of microbiological samples even further. In a first report on secondary isotope imaging spectroscopy combined with FISH, physiological processes and cell identity were analysed in marine anoxic communities at the bacterial cell level (Orphan *et al.*, 2001). An overview of the secondary-ion mass spectrometry (SIMS) technique and its application in biology/microbiology was provided by the group of Lechene *et al.* (2006). The technique, also known as nanoSIMS, has already been applied in combination with various FISH techniques in order to link bacterial identity with function (see Table 3 for abbreviations and details). Some very recent studies examined cocultures by EL-FISH/nanoSIMS (Behrens *et al.*, 2008), microbial mats and sulphur cycling by CARD-FISH/nanoSIMS (Fike *et al.*, 2008), a proof-of-principle study using cocultures by SIMSISH (Li *et al.*, 2008), anaerobic phototrophic bacteria and their ecophysiology by HISH/SIMS (Musat *et al.*, 2008) and the fixation and fate of C and N in cyanobacteria by TEM/nanoSIMS (Finzi-Hart *et al.*, 2009). The current state of the art in SIMS imaging has been reviewed by Wagner (2009). Obviously, there is ongoing development of a plethora of correlative high-resolution imaging techniques, all of which will further expand our knowledge of the structure and metabolism of microbial communities at the single-cell level.

## Acknowledgements

This work was supported by the Helmholtz Centre for Environmental Research – UFZ and the DAAD (Germany), Environment Canada, the Advanced Foods and Materials Network, NSERC (Canada) and the Canada Research Chair program (A.P.H.). The STXM5.3.2 microscope was constructed from funds supplied by the Department of Energy, NSF, Dow Chemical, NSERC and the Canada Foundation for Innovation. Its operation is supported by DOE-BES. We thank David Kilcoyne and Tolek Tyliszczak for their outstanding contributions to developing and maintaining the instrument. The Advanced Light Source is supported by the Director, Office of Energy Research, Office of Basic Energy Sciences, Materials Sciences Division of the US Department of Energy, under contract no. DE-AC03-76SF00098. The Canadian Light Source is supported by NSERC, CFI and the University of Saskatchewan.

## References

- Abragam A (1961) *The Principles of Nuclear Magnetism*. Clarendon Press, Oxford.

- Ade H & Hitchcock AP (2008) NEXAFS microscopy and resonant scattering: composition and orientation probed in real and reciprocal space. *Polymer* **49**: 643–675.
- Ade H & Urquhart SG (2002) NEXAFS spectroscopy and microscopy of natural and synthetic polymers. *Chemical Applications of Synchrotron Radiation* (Sham TK, ed), pp. 285–355. World Scientific Publishing, Singapore.
- Alfreider A, Pernthaler J, Amann R, Sattler B, Glöckner F-O, Wille A & Psenner R (1996) Community analysis of the bacterial assemblages in the winter cover and pelagic layers of a high mountain lake by *in situ* hybridization. *Appl Environ Microb* **62**: 2138–2144.
- Amann R, Ludwig W & Schleifer K (1995) Phylogenetic identification and *in situ* detection of individual microbial cells without cultivation. *Microbiol Rev* **59**: 143–169.
- Assmus B, Schloter M, Kirchhof G, Hutzler P & Hartmann A (1997) Improved *in situ* tracking of rhizosphere bacteria using dual staining with fluorescence-labeled antibodies and rRNA-targeted oligonucleotides. *Microb Ecol* **33**: 32–40.
- Bahlmann K, Jakobs S & Hell SW (2001) 4Pi-confocal microscopy of live cells. *Ultramicroscopy* **87**: 155–164.
- Bartosch S, Wolgast I, Spieck E & Bock E (1999) Identification of nitrite-oxidizing bacteria with monoclonal antibodies recognizing the nitrite oxidoreductase. *Appl Environ Microb* **65**: 4126–4133.
- Bates M, Huang B, Dempsey GT & Zhuang X (2007) Multicolor super-resolution imaging with photo-switchable fluorescent probes. *Science* **317**: 1749–1753.
- Behrens S, Lösekann T, Pett-Ridge J, Weber PK, Ng W-O, Stevensen BS, Hutcheon ID, Relman DA & Spormann AM (2008) Linking microbial phylogeny to metabolic activity at the single-cell level by using enhanced element labelling-catalyzed reporter deposition fluorescence *in situ* hybridisation (EL-FISH) and nanoSIMS. *Appl Environ Microb* **74**: 3143–3150.
- Benzerara K, Yoon TH, Tyliszczak T, Constantz B, Spormann AM & Brown GE (2004) Scanning transmission X-ray microscopy study of microbial calcification. *Geobiology* **2**: 249–259.
- Benzerara K, Yoon T-H, Menguy N, Tyliszczak T & Brown GE Jr (2005) Nanoscale environments associated with bioweathering of a Mg–Fe-pyroxene. *P Natl Acad Sci USA* **102**: 979–982.
- Benzerara K, Menguy N, López-García P, Yoon T-H, Kazmierczak J, Tyliszczak T, Guyot F & Brown GE Jr (2006) Nanoscale detection of organic signatures in carbonate microbialites. *P Natl Acad Sci USA* **103**: 9440–9445.
- Beuling EE, van Dusschoten D, Lens P, van den Heuvel JC, Van As H & Ottengraf SPP (1998) Characterization of the diffusive properties of biofilms using pulsed field gradient-nuclear magnetic resonance. *Biotechnol Bioeng* **60**: 283–291.
- Bewersdorf J, Bennett BT & Knight KL (2006) H2AX chromatin structures and their response to DNA damage revealed by 4pi microscopy. *P Natl Acad Sci USA* **103**: 18137–18142.
- Binning G, Rohrer H, Gerber C & Weibel E (1982) Surface studies by scanning tunneling microscopy. *Phys Rev Lett* **49**: 57–61.
- Blazejak A, Erseus C, Amann R & Dubilier N (2005) Coexistence of bacterial sulfide oxidizers, sulfate reducers, and spirochetes in a gutless worm (oligochaeta) from the Peru margin. *Appl Environ Microb* **71**: 1553–1561.
- Bloch F, Hansen WW & Packard M (1946) The nuclear induction experiment. *Phys Rev* **70**: 474–485.
- Bluhm H, Andersson K, Araki T et al. (2005) Soft X-ray microscopy and spectroscopy at the molecular environmental science beamline at the advanced light source. *J Electron Spectrosc* **150**: 86–104.
- Callaghan PT (1991) *Principles of Nuclear Magnetic Resonance Microscopy*. Clarendon Press, Oxford.
- Callaghan PT & Xia Y (1991) Velocity and diffusion imaging in dynamic NMR microscopy. *J Magn Reson* **91**: 326–352.
- Chalmers NI, Palmer RJ Jr, Du-Thumm L, Sullivan R, Shi W & Kolenbrander PE (2007) Use of quantum dot luminescent probes to achieve single-cell resolution of human oral bacteria in biofilms. *Appl Environ Microb* **73**: 630–636.
- Chan CS, De Stasio G, Welch SA, Girasole M, Frazer BH, Nesterova MV, Fakra S & Banfield JF (2004) Microbial polysaccharides template assembly of nanocrystal fibers. *Science* **303**: 1656–1658.
- Chao WL, Harteneck BD, Liddle JA, Anderson EH & Attwood DT (2005) Soft X-ray microscopy at a spatial resolution better than 15 nm. *Nature* **435**: 1210–1213.
- Christensen BB, Sternberg C, Andersen JB, Palmer RB Jr, Toftgaard Nielsen A, Givskov M & Molin S (1999) Molecular tools for study of biofilm physiology. *Method Enzymol* **310**: 20–42.
- Clegg RM, Holub O & Gohlke C (2003) Fluorescence lifetime-resolved imaging: measuring lifetimes in an image. *Method Enzymol* **360**: 509–542.
- Dazzo FB, Schmid M & Hartmann A (2007) Immunofluorescence microscopy and fluorescence *in situ* hybridisation combined with CMEIAS and other image analysis tools for soil- and plant-associated microbial autecology. *Manual of Environmental Microbiology* (Hurst CJ, Crawford RL, Garland JL, Lipson DA, Mills AL & Stetzenbach LD, eds), pp. 712–733. ASM, Washington, DC.
- Decho AW & Kawaguchi T (1999) Confocal imaging of *in situ* natural microbial communities and their extracellular polymeric secretions using Nanoplast resin. *BioTechniques* **27**: 1246–1252.
- DeLong EF, Taylor LT, Marsh TL & Preston CM (1999) Visualization and enumeration of marine planktonic archaea and bacteria by using polyribonucleotide probes and fluorescent *in situ* hybridization. *Appl Environ Microb* **65**: 5554–5563.
- Donnert G, Keller J, Medda R, Andrei MA, Rizzoli SO, Lührmann R, Jahn R, Eggeling C & Hell SW (2006) Macromolecular-scale resolution in biological fluorescence microscopy. *P Natl Acad Sci USA* **103**: 11440–11445.
- Dynes JJ, Lawrence JR, Korber DR, Swerhone GDW, Leppard GG & Hitchcock AP (2006a) Quantitative mapping of chlorhexidine in natural river biofilms. *Sci Total Environ* **369**: 369–383.
- Dynes JJ, Tyliszczak T, Araki T, Lawrence JR, Swerhone GDW, Leppard GG & Hitchcock AP (2006b) Speciation and

- quantitative mapping of metal species in microbial biofilms using scanning transmission X-ray microscopy. *Environ Sci Technol* **40**: 1556–1565.
- Errampalli D, Leung K, Cassidy MB, Krostrzynska M, Blears M, Lee H & Trevors JT (1999) Application of the green fluorescent protein as a molecular marker in environmental microorganisms. *J Microbiol Meth* **35**: 187–199.
- Ferrari BC, Tujula N, Stoner K & Kjelleberg S (2006) Catalyzed reporter deposition-fluorescence *in situ* hybridization allows for enrichment-independent detection of microcolony-forming soil bacteria. *Appl Environ Microb* **72**: 918–922.
- Fike DA, Gammon CL, Ziebis W & Orphan VJ (2008) Micro-scale mapping of sulphur cycling across the oxycline of a cyanobacterial mat: a paired nanoSIMS and CARD-FISH approach. *ISME J* **2**: 749–759.
- Finzi-Hart JA, Pett-Ridge J, Weber PK, Popa R, Fallon SJ, Gunderson T, Hutcheon ID, Nealon KH & Capone DG (2009) Fixation and fate of C and N in the cyanobacterium *Trichodesmium* using nanometer-scale secondary ion mass spectrometry. *P Natl Acad Sci USA* **106**: 6345–6350.
- Flemming H-C, Neu TR & Wozniak D (2007) The EPS matrix: the “house of biofilm cells”. *J Bacteriol* **189**: 7945–7947.
- Gerritsen HC, Draaijer A, van den Heuvel DJ & Agronskaia AV (2006) Fluorescence lifetime imaging in scanning microscopy. *Handbook of Biological Confocal Microscopy* (Pawley JB, eds), pp. 516–534. Springer, New York.
- Gilbert B, Assmus B, Hartmann A & Frenzel P (1998) *In situ* localization of two methanotrophic strains in the rhizosphere of rice plants. *FEMS Microbiol Ecol* **25**: 117–128.
- Gilbert ES, Khlebnikov A, Meyer-Ilse W & Keasling JD (1999) Use of soft X-ray microscopy for the analysis of early-stage biofilm formation. *Water Sci Technol* **39**: 269–272.
- Gjersing EL, Codd SL, Seymour JD & Stewart PS (2005) Magnetic resonance microscopy analysis of advective transport in a biofilm reactor. *Biotechnol Bioeng* **89**: 822–834.
- Graf von der Schulenburg DA, Holland DJ, Paterson-Beedle M, Macaskie LE, Gladden LF & Johns ML (2008a) Spatially resolved quantification of metal ion concentration in a biofilm-mediated ion exchanger. *Biotechnol Bioeng* **99**: 821–829.
- Graf von der Schulenburg DA, Akpa BS, Gladden LF & Johns ML (2008b) Non-invasive mass transfer measurements in complex biofilm-coated structures. *Biotechnol Bioeng* **101**: 602–608.
- Gray ND, Howarth R, Pickup RW, Jones JG & Head IM (2000) Use of combined microautoradiography and fluorescence *in situ* hybridization to determine carbon metabolism in mixed natural communities of uncultured from the genus *Achromatium*. *Appl Environ Microb* **66**: 4518–4522.
- Greenfield D, McEvoy AL, Shroff H, Crooks GE, Wingreen NS, Betzig E & Liphardt J (2009) Self-organisation of the *Escherichia coli* chemotaxis network imaged with super-resolution light microscopy. *PLoS Biol* **7**: 1–11.
- Gu F, Lux R, Du-Thumm L, Stokes I, Kreth J, Anderson MH, Wong DT, Wolinsky L, Sullivan R & Shi W (2005) *In situ* and non-invasive detection of specific bacterial species in oral biofilms using fluorescently labelled monoclonal antibodies. *J Microbiol Meth* **62**: 145–160.
- Gustafsson MGL (2000) Surpassing the lateral resolution limit by a factor of two using structured illumination microscopy. *J Microscopy* **198**: 82–87.
- Haisch C & Niessner R (2007) Visualisation of transient processes in biofilms by optical coherence tomography. *Water Res* **41**: 2467–2472.
- Haugland RP (2005) *A Guide to Fluorescent Probes and Labelling Techniques*. Invitrogen Corp., Carlsbad, CA, USA.
- Hell SW (2007) Far-field optical nanoscopy. *Science* **316**: 1153–1158.
- Hell SW (2009) Microscopy and its focal switch. *Nat Methods* **6**: 24–32.
- Hess ST, Girirajan TPK & Mason MD (2006) Ultra-high resolution imaging by fluorescence photoactivation localization microscopy. *Biophys J* **91**: 4258–4272.
- Hinck S, Neu TR, Lavik G, Mußmann M, de Beer D & Jonkers HM (2007) Physiological adaptation of nitrate storing *Beggiatoa* to diel cycling in a phototrophic hypersaline mat. *Appl Environ Microb* **73**: 7013–7022.
- Hitchcock AP (2008) aXis2000 is written in Interactive Data Language (IDL) and available free for non-commercial use. Available at <http://unicorn.mcmaster.ca/aXis2000.html>
- Hitchcock AP, Morin C, Zhang X, Araki T, Dynes JJ, Stöver H, Brash JL, Lawrence JR & Leppard GG (2005) Soft X-ray spectromicroscopy of biological and synthetic polymer systems. *J Electron Spectrosc* **144–147**: 259–269.
- Holst G & Grunwald B (2000) Luminescence lifetime imaging with transparent oxygen optodes. *Sensor Actuat B-Chem* **3664**: 1–13.
- Horn H (2003) *Modellierung von Stoffumsatz und Stofftransport in Biofilmsystemen*. FIT-Verlag, Paderborn.
- Hoskins BC, Fevang L, Majors PD, Sharma MM & Georgiou G (1999) Selective imaging of biofilms in porous media by NMR relaxation. *J Magn Reson* **139**: 67–73.
- Hu Z, Hidalgo G, Houston PL, Hay AG, Shuler ML, Abruna HD, Ghiorse WC & Lion LW (2005) Determination of spatial distribution of zinc and active biomass in microbial biofilms by two-photon laser scanning microscopy. *Appl Environ Microb* **71**: 4014–4021.
- Huang B, Jones SA, Brandenburg B & Zhuang X (2008a) Whole-cell 3D STORM reveals interactions between cellular structures with nanometer-scale resolution. *Nat Methods* **5**: 1047–1052.
- Huang B, Wang W, Bates M & Zhuang X (2008b) Three-dimensional super-resolution imaging by stochastic optical reconstruction microscopy. *Science* **319**: 810–813.
- Huang WE, Stoecker K, Griffiths R, Newbold L, Daims H, Whitley AS & Wagner M (2007) Raman-FISH: combining stable-isotope Raman spectroscopy and fluorescence *in situ* hybridization for the single cell analysis of identity and function. *Environ Microbiol* **9**: 1878–1889.
- Jacobsen C (2006) Analysis routines written in IDL. Available at <http://xray1.physics.sunysb.edu/data/>

- Jacobsen C, Wirick S, Flynn G & Zimba C (2000) Soft X-ray spectroscopy from image sequences with sub-100 nm spatial resolution. *J Microscopy* **197**: 173–184.
- Jacobsen C, Feser M, Lerotic M, Vogt S, Maser J & Schäfer T (2003) Cluster analysis of soft x-ray spectromicroscopy data. *J Phys IV France* **104**: 623–626.
- Janssen JK (2003) Marker and reporter genes: illuminating tools for environmental microbiologists. *Curr Opin Microbiol* **6**: 310–316.
- Kawaguchi T & Decho A (2002) *In situ* microspatial imaging using two-photon and confocal laser scanning microscopy of bacteria and extracellular polymeric secretions (EPS) within marine stromatolites. *Mar Biotechnol* **4**: 127–131.
- Kaznatcheev KV, Karunakaran C, Lanke UD, Urquhart SG, Obst M & Hitchcock AP (2007) Soft X-ray spectromicroscopy beamline at the CLS: commissioning results. *Nucl Instrum Methods A* **582**: 96–99.
- Kemner KM, Kelly SD, Lai B, Maser J, O'Loughlin EJ, Sholto-Douglas D, Cai Z, Schneegurt MA, Kulpa CF Jr & Neelson KH (2004) Elemental and redox analysis of single bacterial cells by X-ray microbeam analysis. *Science* **306**: 686–687.
- Kilcoyne ALD, Steele WE, Fakra S *et al.* (2003) Interferometrically controlled scanning transmission microscopes at the advanced light source. *J Synchrotron Radiat* **10**: 125–136.
- Kirz J & Rarback H (1985) Soft X-ray microscopes. *Rev Sci Instrum* **56**: 1–13.
- Kirz J, Jacobsen C & Howells M (1995) Soft X-ray microscopes and their biological applications. *Q Rev Biophys* **28**: 33–130.
- Klar TA, Jakobs S, Dyba M, Egner A & Hell SW (2000) Fluorescence microscopy with diffraction resolution barrier broken by stimulated emission. *P Natl Acad Sci USA* **97**: 8206–8210.
- Klausen M, Aaes-Jørgensen A, Molin S & Tolker-Nielsen T (2003) Involvement of bacterial migration in the development of complex multicellular structures in *Pseudomonas aeruginosa* biofilms. *Mol Microbiol* **50**: 61–68.
- Kubota K, Ohashi A, Imachi H & Harada H (2006) Improved *in situ* hybridization efficiency with locked-nucleic-acid-incorporated DNA probes. *Appl Environ Microb* **72**: 5311–5317.
- Kühl M, Rickelt LF & Thar R (2007) Combined imaging of bacteria and oxygen in biofilms. *Appl Environ Microb* **73**: 6289–6295.
- La Heij EJ, Kerkof PJAM, Kopinga K & Pel L (1996) Determining porosity profiles during filtration and expression of sewage sludge by NMR imaging. *AIChE J* **42**: 953–959.
- Larrainzar E, O'Gara F & Morrissey JP (2005) Applications of autofluorescent proteins for *in situ* studies in microbial ecology. *Annu Rev Microbiol* **59**: 257–277.
- Lauterbur PC (1973) Image formation by induced local interactions: examples employing nuclear magnetic resonance. *Nature* **242**: 190–191.
- Lawrence JR & Neu TR (1999) Confocal laser scanning microscopy for analysis of microbial biofilms. *Method Enzymol* **310**: 131–144.
- Lawrence JR & Neu TR (2007a) Laser scanning microscopy for microbial flocs and particles. *Environmental Colloids: Behavior, Structure and Characterization* (Wilkinson KJ & Lead JR, eds), pp. 469–505. John Wiley, New York, NY.
- Lawrence JR & Neu TR (2007b) Laser scanning microscopy. *Methods for General and Molecular Microbiology* (Reddy CA, Beveridge TJ, Breznak JA, Marzluf GA, Schmidt TM & Snyder LR, eds), pp. 34–53. ASM, Washington, DC.
- Lawrence JR, Korber DR, Hoyle BD, Costerton JW & Caldwell DE (1991) Optical sectioning of microbial biofilms. *J Bacteriol* **173**: 6558–6567.
- Lawrence JR, Wolfaardt GM & Korber DR (1994) Monitoring diffusion in biofilm matrices using scanning confocal microscopy. *Appl Environ Microb* **60**: 1166–1173.
- Lawrence JR, Wolfaardt G & Neu TR (1998) The study of microbial biofilms by confocal laser scanning microscopy. *Digital Image Analysis of Microbes* (Wilkinson MHF & Shut F, eds), pp. 431–465. Wiley, Chichester, UK.
- Lawrence JR, Swerhone GDW, Leppard GG, Araki T, Zhang X, West MM & Hitchcock AP (2003) Scanning transmission X-ray, laser scanning, and transmission electron microscopy mapping of the exopolymeric matrix of microbial biofilms. *Appl Environ Microb* **69**: 5543–5554.
- Lawrence JR, Hitchcock AP, Leppard GG & Neu TR (2005) Mapping biopolymer distributions in microbial communities. *Flocculation in Natural and Engineered Environmental Systems* (Droppo IG, Leppard GG, Liss SN & Milligan TM, eds), pp. 121–141. CRC Press, Boca Raton, FL.
- Lawrence JR, Korber DR & Neu TR (2007a) Analytical imaging and microscopy techniques. *Manual of Environmental Microbiology* (Hurst CJ, Crawford RL, Garland JL, Lipson DA, Mills AL & Stetzenbach LD, eds), pp. 40–68. ASM, Washington, DC.
- Lawrence JR, Swerhone GDW & Neu TR (2007b) *In situ* evidence for microdomains in the polymer matrix of bacterial microcolonies. *Can J Microbiol* **53**: 450–458.
- Lechene C, Hillion F, McMahon G *et al.* (2006) High-resolution quantitative imaging of mammalian and bacterial cells using stable isotope mass spectrometry. *J Biol* **5**: 20.
- Lee N, Nielsen PH, Andreasen KH, Juretschko S, Nielsen JL, Schleifer K & Wagner M (1999) Combination of fluorescent *in situ* hybridisation and microautoradiography – a new tool for structure-function analyses in microbial ecology. *Appl Environ Microb* **65**: 1289–1297.
- Lehtola MJ, Torvinen E, Miettinen IT & Keevil CW (2006) Fluorescence *in situ* hybridisation using peptide nucleic acid probes for rapid detection of *Mycobacterium avium* subsp. *avium* and *Mycobacterium avium* subsp. *paratuberculosis* in potable-water biofilms. *Appl Environ Microb* **72**: 848–853.
- Lens PNL & van As H (2003) Use of <sup>1</sup>H NMR to study transport processes in biofilms. *Biofilms in Medicine, Industry and Environmental Biotechnology: Characteristics, Analysis and Control* (Lens P, Moran AP, Mahony T, Stoodley P & O'Flaherty V, eds), pp. 285–307. IWA Publishing, London.

- Lerotic M, Jacobsen C, Schäfer T & Vogt S (2004) Cluster analysis of soft x-ray spectromicroscopy data. *Ultramicroscopy* **100**: 35–45.
- Lerotic M, Jacobsen C, Gillow JB, Francis AJ, Wirick S, Vogt S & Maser J (2005) Cluster analysis in soft X-ray spectromicroscopy: finding the patterns in complex specimens. *J Electron Spectrosc* **144–147**: 1137–1142.
- Leveau JHJ & Lindow SE (2002) Bioreporters in microbial ecology. *Curr Opin Microbiol* **5**: 259–265.
- Lewandowski Z, Altobelli SA & Fukushima E (1993) NMR and microelectrode studies of hydrodynamics and kinetics in biofilms. *Biotechnol Progr* **9**: 40–45.
- Li T, Wu T-D, Mazeas L, Toffin L, Guerquin-Kern J-L, Leblon G & Bouchez T (2008) Simultaneous analysis of microbial identity and function using nanoSIMS. *Environ Microbiol* **10**: 580–588.
- Liebsch G, Klimant I, Frank B, Holst G & Wolfbeis OS (2000) Luminescence lifetime imaging of oxygen, pH, and carbon dioxide distribution using optical sensors. *Appl Spectrosc* **54**: 548–559.
- Mansfield P & Grannell PK (1973) NMR 'diffraction' in solids? *J Phys C Solid State* **6**: L422–L426.
- Mansfield P & Morris PG (1982) *NMR Imaging in Biomedicine*. Academic Press, New York.
- Manz B (2004) Combined relaxation and displacement experiment (COMRADE): a fast method to acquire T2, diffusion and velocity maps. *J Magn Reson* **169**: 60–67.
- Manz B & Callaghan PT (1997) NMR investigations of self-diffusion and shear thinning for semidilute polymer solutions near the demixing transition. *Macromolecules* **30**: 3309–3316.
- Manz B, Alexander P, Warren PB & Gladden LF (1998) Characterisation of fluid flow through porous media using three-dimensional microimaging and pulsed gradient stimulated echo NMR. *Magn Reson Imaging* **16**: 673–676.
- Manz B, Alexander P & Gladden LF (1999a) Correlations between dispersion and structure in porous media probed by NMR. *Phys Fluids* **11**: 259–267.
- Manz B, Warren PB & Gladden LF (1999b) Flow and dispersion in porous media: Lattice-Boltzmann and NMR studies. *AIChE J* **45**: 1845–1854.
- Manz B, Volke F, Goll D & Horn H (2003) Measuring local flow velocities and biofilm structure in biofilm systems with Magnetic Resonance Imaging (MRI). *Biotechnol Bioeng* **84**: 424–432.
- Manz B, Volke F, Goll D & Horn H (2005) Investigation of biofilm structure, flow patterns and detachment with Magnetic Resonance Imaging (MRI). *Water Sci Technol* **52**: 1–6.
- Manz B, Neu TR, Volke F, Staudt C, Haesner M, Hempel DC & Horn H (2006) Application of MRI and CLSM for the analysis of biofilm detachment. *Fouling, Cleaning & Disinfection in Food Processing, Proceedings* (Wilson DI, Chew JYM, Fryer PJ & Hastings APM, eds), pp. 64–70. Jesus College, Cambridge, UK.
- Manz W, Arp G, Schumann-Kindel G, Szwedzyk U & Reitner J (2000) Widefield deconvolution epifluorescence microscopy combined with fluorescence *in situ* hybridization reveals the spatial arrangement of bacteria in sponge tissue. *J Microbiol Meth* **40**: 125–134.
- McLean JS, Ona ON & Majors PD (2008) Correlated biofilm imaging, transport and metabolism measurements via combined nuclear magnetic resonance and confocal microscopy. *ISME J* **2**: 121–131.
- McRobbie DW, Moore EA, Graves MJ & Prince MA (2006) *MRI from Picture to Proton*. Cambridge University Press, Cambridge.
- Metzger U, Lankes U, Hardy EH, Gordalla BC & Frimmel FH (2006) Monitoring the formation of an *Aureobasidium pullulans* biofilm in a bead-packed reactor via flow-weighted magnetic resonance imaging. *Biotechnol Lett* **28**: 1305–1311.
- Molin S & Givskov M (1999) Application of molecular tools for *in situ* monitoring of bacterial growth activity. *Environ Microbiol* **1**: 383–391.
- Moter A & Göbel UB (2000) Fluorescence *in situ* hybridization (FISH) for direct visualization of microorganisms. *J Microbiol Meth* **41**: 85–112.
- Musat N, Halm H, Winterholler B, Hoppe P, Peduzzi S, Hillion F, Horreard F, Amann R, Jörgensen BB & Kuypers MMM (2008) A single-cell view on the ecophysiology of anaerobic phototrophic bacteria. *P Natl Acad Sci USA* **105**: 17861–17866.
- Neu TR & Lawrence JR (1999) Lectin-binding-analysis in biofilm systems. *Method Enzymol* **310**: 145–152.
- Neu TR & Lawrence JR (2002) Laser scanning microscopy in combination with fluorescence techniques for biofilm study. *The Encyclopedia of Environmental Microbiology* (Bitton G, ed), pp. 1772–1788. John Wiley, New York, NY.
- Neu TR & Lawrence JR (2005) One-photon versus two-photon laser scanning microscopy and digital image analysis of microbial biofilms. *Method Microbiol* **34**: 87–134.
- Neu TR, Swerhone GDW & Lawrence JR (2001) Assessment of lectin-binding analysis for *in situ* detection of glycoconjugates in biofilm systems. *Microbiology* **147**: 299–313.
- Neu TR, Kuhlicke U & Lawrence JR (2002) Assessment of fluorochromes for two-photon laser scanning microscopy of biofilms. *Appl Environ Microb* **68**: 901–909.
- Neu TR, Walczysko P & Lawrence JR (2004a) Two-photon imaging for studying the microbial ecology of biofilm systems. *Microb Environ* **19**: 1–6.
- Neu TR, Woelfl S & Lawrence JR (2004b) Three-dimensional differentiation of photo-autotrophic biofilm constituents by multi-channel laser scanning microscopy (single-photon and two-photon excitation). *J Microbiol Meth* **56**: 161–172.
- Nielsen JL, Wagner M & Nielsen PH (2003) Use of microautoradiography to study *in situ* physiology of bacteria in biofilms. *Rev Environ Sci Bio/Technol* **2**: 261–268.
- Not F, Simon N, Biegala IC & Vaulot D (2002) Application of fluorescent *in situ* hybridization coupled with tyramide signal amplification (FISH-TSA) to assess eucaryotic picoplankton composition. *Aquat Microb Ecol* **28**: 157–166.
- Nott KP, Heese FP, Hall LD, Macaskie LE & Paterson-Beedle M (2005) Measurement of flow field in biofilm reactors by 3-D magnetic resonance imaging. *AIChE J* **51**: 3072–3079.

- Okabe S, Kindaichi T & Ito T (2005) Fate of  $^{14}\text{C}$ -labeled microbial products derived from nitrifying bacteria in autotrophic nitrifying biofilms. *Appl Environ Microb* **71**: 3987–3994.
- Orphan VJ, House CH, Hinrichs KU, McKeegan KD & De Long EF (2001) Methane-consuming archaea revealed by directly coupled isotopic and phylogenetic analysis. *Science* **293**: 484–487.
- Palmer RJ Jr, Haagensen J, Neu TR & Sternberg C (2006) Confocal microscopy of biofilms – spatiotemporal approaches. *Handbook of Biological Confocal Microscopy* (Pawley JB, ed), pp. 882–900. Springer, New York, NY.
- Pecher K, McCubbery D, Kneedler E, Rothe J, Bargar J, Meigs G, Cox L, Neelson K & Tonner B (2003) Quantitative charge state analysis of manganese biominerals in aqueous suspension using Scanning Transmission X-ray Microscopy (STXM). *Geochim Cosmochim Acta* **67**: 1089–1098.
- Pernthaler A, Pernthaler J & Amann R (2002) Fluorescence *in situ* hybridisation and catalyzed reporter deposition for the identification of marine bacteria. *Appl Environ Microb* **68**: 3094–3101.
- Perry-O’Keefe H, Rigby S, Oliveira K, Sørensen D, Stender H, Coull J & Hyldig-Nielsen JJ (2001) Identification of indicator microorganisms using a standardized PNA FISH method. *J Microbiol Meth* **47**: 281–292.
- Phillips GJ (2001) Green fluorescent protein – a bright idea for the study of bacterial protein localization. *FEMS Microbiol Lett* **204**: 9–18.
- Phipps D, Rodriguez G & Ridgway H (1999) Deconvolution fluorescence microscopy for observation and analysis of membrane biofilm architecture. *Method Enzymol* **310**: 178–194.
- Phoenix VR & Holmes WM (2008) Magnetic resonance imaging of structure, diffusivity and copper immobilisation in a phototrophic biofilm. *Appl Environ Microb* **74**: 4934–4943.
- Pinck C, Coeur C, Potier P & Bock E (2001) Polyclonal antibodies recognizing the AmoB Protein of ammonia oxidizers of the  $\beta$ -subclass of the class *Proteobacteria*. *Appl Environ Microb* **67**: 118–124.
- Potter K, Kleinberg RL, Brockman FJ & McFarland EW (1996) Assay for bacteria in porous media by diffusion-weighted NMR. *J Magn Reson Ser B* **113**: 9–15.
- Pratscher J, Stichternoth C, Fichtl K, Schleifer K-H & Braker G (2009) Application of recognition of individual genes-fluorescence *in situ* hybridisation (Ring-FISH) to detect nitrite reductase genes (*nirK*) of denitrifiers in pure cultures and environmental samples. *Appl Environ Microb* **75**: 802–810.
- Purcell EM, Torrey HC & Pound RV (1946) Resonance absorption by nuclear magnetic moments in a solid. *Phys Rev* **69**: 37–38.
- Rinck PA (2001) *Magnetic Resonance in Medicine*. Blackwell Publishing, Berlin.
- Rust MJ, Bates M & Zhuang X (2006) Sub-diffraction-limit imaging by stochastic optical reconstruction microscopy (STORM). *Nat Methods* **3**: 793–796.
- Sayler GS & Layton AC (1990) Environmental application of nucleic acid hybridization. *Annu Rev Microbiol* **44**: 625–648.
- Schlöter M, Borlinghaus R, Bode W & Hartmann A (1993) Direct identification, and localization of *Azospirillum* in the rhizosphere of wheat using fluorescence-labelled monoclonal antibodies and confocal scanning laser microscopy. *J Microscopy* **171**: 173–177.
- Schlöter M, Wiehe W, Assmus B, Steindl H, Becke H, Höflich G & Hartmann A (1997) Root colonization of different plants by plant-growth-promoting *Rhizobium leguminosarum* bv. *trifolii* R39 studied with monospecific polyclonal antisera. *Appl Environ Microb* **63**: 2038–2046.
- Schmid M, Rothballer M, Assmus B, Hutzler P, Lawrence JR, Schlöter M & Hartmann A (2004) Detection of microbes by scanning confocal laser microscopy (SCLM). *Molecular Microbial Ecology Manual* (Kowalchuk GA, de Bruijn FJ, Head IM, Akkermans ADL & van Elsas JD, eds), pp. 875–910. Kluwer Academic Publishers, Dordrecht, the Netherlands.
- Schmid M, Selesi D, Rothballer M, Schlöter M, Lee N, Kandler E & Hartmann A (2006) Localization and visualisation of microbial community structure and activity in soil microhabitats. *Intestinal microorganisms of termites and other invertebrates, Vol. 6* (König H & Varma A, eds), pp. 439–461. Springer-Verlag, Berlin, Germany.
- Schönhuber W, Fuchs B, Juretschko S & Amann R (1997) Improved sensitivity of whole-cell hybridization by the combination of horseradish peroxidase-labeled oligonucleotides and tyramide signal amplification. *Appl Environ Microb* **63**: 3268–3273.
- Schönhuber M, Zarda B, Eix S, Rippka R, Herdmann M, Ludwig W & Amann R (1999) *In situ* identification of cyanobacteria with horseradish peroxidase-labeled, rRNA-targeted oligonucleotide probes. *Appl Environ Microb* **65**: 1259–1267.
- Schrader M, Bahlmann K, Giese G & Hell SW (1998) 4pi-confocal imaging in fixed biological specimens. *Biophys J* **75**: 1659–1668.
- Schramm A, Fuchs BM, Nielsen JL, Tonolla M & Stahl DA (2002) Fluorescence *in situ* hybridization of 16S rRNA gene clones (Clone-FISH) for probe validation and screening of clone libraries. *Environ Microbiol* **4**: 713–720.
- Sekar R, Pernthaler A, Warnecke F, Posch T & Amann R (2003) An improved protocol for quantification of freshwater *Actinobacteria* by fluorescence *in situ* hybridization. *Appl Environ Microb* **69**: 2928–2935.
- Seymour JD, Manz B & Callaghan PT (1999) Pulsed gradient spin echo NMR measurements of hydrodynamic instabilities with coherent structure: Taylor vortices. *Phys Fluids* **11**: 1104–1113.
- Seymour JD, Gage JP, Codd SL & Gerlach R (2004a) Anomalous fluid transport in porous media induced by biofilm growth. *Phys Rev Lett* **93**: 198103-1–198103-4.
- Seymour JD, Codd SL, Gjersing EL & Stewart PS (2004b) Magnetic resonance microscopy of biofilm structure and impact on transport in a capillary bioreactor. *J Magn Reson* **167**: 322–327.

- Shermelleh L, Carlton PM, Haase S *et al.* (2008) Subdiffraction multicolour imaging of the nuclear periphery with 3D structured illumination microscopy. *Science* **320**: 1332–1336.
- Shroff H, Galbraith CG, Galbraith JA, White H, Gillette J, Olenych S, Davidson MW & Betzig E (2007) Dual-color superresolution imaging of genetically expressed probes within individual adhesion complexes. *P Natl Acad Sci USA* **104**: 20308–20313.
- Shroff H, Galbraith CG, Galbraith JA & Betzig E (2008) Live-cell photoactivated localization microscopy of nanoscale adhesion dynamics. *Nat Methods* **5**: 417–423.
- Sintes E & Herndl GJ (2006) Quantifying substrate uptake by individual cells of marine bacterioplankton by catalyzed reporter deposition fluorescence *in situ* hybridization combined with microautoradiography. *Appl Environ Microb* **72**: 7022–7028.
- Slichter CP (1990) *Principles of Magnetic Resonance*. Springer-Verlag, Heidelberg.
- Staudt C, Horn H, Hempel DC & Neu TR (2003) Screening of lectins for staining lectin-specific glycoconjugates in the EPS of biofilms. *Biofilms in Medicine, Industry and Environmental Technology* (Lens P, Moran AP, Mahony T, Stoodley P & O'Flaherty V, eds), pp. 308–327. IWA Publishing, UK.
- Stejskal EO & Tanner JE (1965) Spin diffusion measurements: spin echoes in the presence of a time-dependent field gradient. *J Chem Phys* **42**: 288–292.
- Stender H, Kurtzmann C, Hyldig-Nielsen JJ, Sørensen D, Broome A, Oliveira K, Perry-O'Keefe H, Sage A, Young B & Coull J (2001) Identification of *Dekkera bruxellensis* (*Brettanomyces*) from wine by fluorescence *in situ* hybridisation using peptide nucleic acid probes. *Appl Environ Microb* **67**: 938–941.
- Thomsen R, Stein Nielsen P & Heick Jensen T (2005) Dramatically improved RNA *in situ* hybridisation signals using LNA-modified probes. *RNA* **11**: 1745–1748.
- Tolker-Nielsen T, Brinch UC, Ragas PC, Andersen JB, Suhr Jacobsen C & Molin S (2000) Development and dynamics of *Pseudomonas* sp. biofilms. *J Bacteriol* **182**: 6482–6489.
- Toner B, Fakra S, Villalobos M, Warwick T & Sposito G (2005) Spatially resolved characterization of biogenic manganese oxide production within a bacterial biofilm. *Appl Environ Microb* **71**: 1300–1310.
- Tujula NA, Holmström C, Mußmann M, Amann R, Kjelleberg S & Crocetti GR (2006) A CARD-FISH protocol for the identification and enumeration of epiphytic bacteria on marine algae. *J Microbiol Meth* **65**: 604–607.
- van As H & Lens P (2001) Use of <sup>1</sup>H NMR to study transport processes in porous biosystems. *J Ind Microbiol Biot* **26**: 43–52.
- van Zandvoort MAMJ, Grauw dCJ, Gerritsen HC, Broers JLV, oude Egbrink MGA, Ramaekers FCS & Slaaf DW (2002) Discrimination of DNA and RNA in cells by a vital fluorescent probe: lifetime imaging of SYTO13 in healthy and apoptotic cells. *Cytometry* **47**: 226–235.
- Verity PG, Beatty TM & Williams SC (1996) Visualization and quantification of plankton and detritus using digital confocal microscopy. *Aquat Microb Ecol* **10**: 55–67.
- Vroom JM, Grauw dCJ, Gerritsen HC, Bradshaw AM, Marsh PD, Watson GK, Birmingham JJ & Allison C (1999) Depth penetration and detection of pH gradients in biofilms by two-photon excitation microscopy. *Appl Environ Microb* **65**: 3502–3511.
- Vyalikh DV, Kirchner A, Danzenbacher S, Dedkov YS, Kade A, Mertig M & Molodtsov SL (2005) Photoemission and near-edge X-ray absorption fine structure studies of the bacterial surface protein layer of *Bacillus sphaericus* NCTC 9602. *J Phys Chem B* **109**: 18620–18627.
- Wagner M (2009) Single cell ecophysiology of microbes as revealed by Raman microspectroscopy or secondary ion mass spectrometry imaging. *Annu Rev Microbiol* **63**: 411–429.
- Wagner M, Horn M & Daims H (2003) Fluorescence *in situ* hybridisation for the identification and characterisation of prokaryotes. *Curr Opin Microbiol* **6**: 302–309.
- Wainwright M (2003) An alternative view of the early history of microbiology. *Adv Appl Microbiol* **52**: 333–355.
- Walczysko P, Kuhlicke U, Knappe S, Cordes C & Neu TR (2008) *In situ* activity of suspended and immobilized microbial communities as measured by Fluorescence Lifetime Imaging. *Appl Environ Microb* **74**: 294–299.
- Ward DM (1989) Molecular probes for analysis of microbial communities. *Structure and Function of Biofilms* (Characklis WG & Wilderer P, eds), pp. 145–163. John Wiley, New York.
- Warwick T, Ade H, Kilcoyne ALD, Kritscher M, Tyliczcak T, Fakra S, Hitchcock AP, Hitchcock P & Padmore HA (2002) A new bend magnet beam line for scanning transmission X-ray microscopy at the advanced light source. *J Synchrotron Radiat* **9**: 254–257.
- Worden AZ, Chisholm SW & Binder BJ (2000) *In situ* hybridisation of *Prochlorococcus* and *Synechococcus* (marine cyanobacteria) spp. with rRNA-targeted peptide nucleic acid probes. *Appl Environ Microb* **66**: 284–289.
- Xi C, Marks D, Schlachter S, Luo W & Boppart SA (2006) High-resolution three-dimensional imaging of biofilm development using optical coherence tomography. *J Biomed Optics* **11**: 034001-1–034001-6.
- Yoon TH, Johnson SB, Benzerara K, Doyle CS, Tyliczcak T, Shun DK & Brown GE Jr (2004) *In situ* characterization of aluminum-containing mineral-microorganism aqueous suspensions using scanning transmission X-ray microscopy. *Langmuir* **20**: 10362–10366.
- Zwirgelmair K, Ludwig W & Schleifer K-H (2003a) Improved fluorescence *in situ* hybridization of individual microbial cells using polynucleotide probes: the network hypothesis. *Syst Appl Microbiol* **26**: 327–337.
- Zwirgelmair K, Ludwig W & Schleifer K-H (2003b) Recognition of individual genes in a single bacterial cell by fluorescence *in situ* hybridization – RING-FISH. *Mol Microbiol* **51**: 89–96.